Spring 5-23-2013

Effects of Temperature on the Kinetic Isotope Effects for Proton and Hydride Transfers in the Active Site Variant of Choline Oxidase Ser101Ala

Rizvan C. Uluisik
Georgia State University, ruluisik1@student.gsu.edu

EFFECTS OF TEMPERATURE ON THE KINETIC ISOTOPE EFFECTS FOR PROTON AND HYDRIDE TRANSFERS IN THE ACTIVE SITE VARIANT OF CHOLINE OXIDASE SER101ALA

by

RIZVAN ULUISIK

Under the Direction of Dr. Giovanni Gadda

ABSTRACT

Choline oxidase catalyzes the oxidation of choline to glycine betaine. The reaction includes betaine aldehyde as an intermediate. FAD is reduced by the alcohol substrate, betaine aldehyde intermediate and oxidized by molecular oxygen to give hydrogen peroxide. In this study, the Ser101Ala variant of choline oxidase was prepared to elucidate the contribution of the hydroxyl group of Ser101 in the proton and hydride transfer reactions for proper preorganization and reorganization of the active site towards quantum mechanical tunneling. The thermodynamic parameters associated with the enzyme-catalyzed OH and CH bond cleavages and the temperature dependence of the associated solvent and substrate kinetic isotope effects were investigated using a stopped-flow spectrophotometer. The proton and hydride transfer have been shown to be occurring via quantum tunneling in CHO-S101A enzyme.

INDEX WORDS: Choline oxidase, Quantum tunneling, Proton transfer, Hydride transfer, Kinetic complexity

EFFECTS OF TEMPERATURE ON THE KINETIC ISOTOPE EFFECTS FOR PROTON AND HYDRIDE TRANSFERS IN THE ACTIVE SITE VARIANT OF CHOLINE OXIDASE SER101ALA

by

RIZVAN ULUISIK

A Thesis Submitted in Partial Fulfillment of the Requirements for the Degree of

Master of Science

in the College of Arts and Sciences

Georgia State University

2013

EFFECTS OF TEMPERATURE ON THE KINETIC ISOTOPE EFFECTS FOR PROTON AND HYDRIDE TRANSFERS IN THE ACTIVE SITE VARIANT OF CHOLINE OXIDASE SER101ALA

by

RIZVAN ULUISIK

Committee Chair: Dr. Giovanni Gadda

Committee: Dr. Donald Hamelberg

Dr. Ivaylo Ivanov

Electronic Version Approved:

Office of Graduate Studies

College of Arts and Sciences

Georgia State University

May 2013

ACKNOWLEDGEMENTS

All of the work performed in this thesis was carried out under the direction of Dr. Giovanni Gadda. From the first day that I joined his group, he has been very supportive, patient, and encouraging throughout my graduate studies. His scientific and editorial advice was essential to the completion of this thesis and has taught me countless lessons and insights that I will use the rest of my life. Thank you so much Dr. Gadda. I want to especially thank my lab mentor Swathi Gannavaram. You are an amazing mentor and a friend. Dr. Donald Hamelberg and Dr. Ivaylo Nikolaev Ivanov, I want to thank you for serving in my thesis committee and also for your insightful discussions and critique on my research work. I am also grateful to Swathi Gannavaram, Cyristal Smitherman, Francesca Salvi and Dr. Elvira Romero for having helpful discussions and providing useful inputs. I extend my gratitude to current and former lab mates and friends, Dr. Hongling Yuan, Dr. Andrea Pennati, Dr. Kevin Francis, Yvette Santos (for her unlimited positive energy), Jacob Ball, Quan Bui, Daniel Ouedraogo, Dan Su and Sandra Hagans, for making this an enjoyable and a good learning experience.

TABLE OF CONTENTS

LIST OF TABLES

LIST OF FIGURES

LIST OF SCHEMES

CHAPTER 1.

INTRODUCTION

1.1 Introduction of Choline Oxidase and the reaction

Choline oxidase catalyzes the oxidation of choline to glycine betaine with betaine aldehyde as intermediate and molecular oxygen as final electron acceptor (*1-3*). The reaction occurs through two subsequent oxidation reactions which are mediated by flavin adenine dinucleotide (FAD) (*1-3*). In the reaction, the alcohol substrate is oxidized to betaine aldehyde which is then hydrated followed by its oxidation to glycine betaine (Figure 1.1) (*3*). Previous studies have revealed the mechanistic, biochemical and structural details of oxidation of choline by choline oxidase. The alcohol substrate is activated by abstraction of hydroxyl proton through a catalytic base with pKa of ~ 7.5 (*1, 3, 4*). The pK_a of the catalytic base was determined by pH profile studies on k_{cat} and k_{cat}/K_m values by using choline and substrate analogs in choline oxidase (*3, 4*). Solvent, substrate and multiple kinetic isotope effects studies with steady-state kinetic approach showed that the abstraction of substrate hydroxyl proton yields the formation of alkoxide species. This activation step has been shown to be mechanistically separated from hydride transfer that occur between the α carbon of substrate and the N(5) atom of flavin. This step is kinetically slower than the proton abstraction (*2-4*).

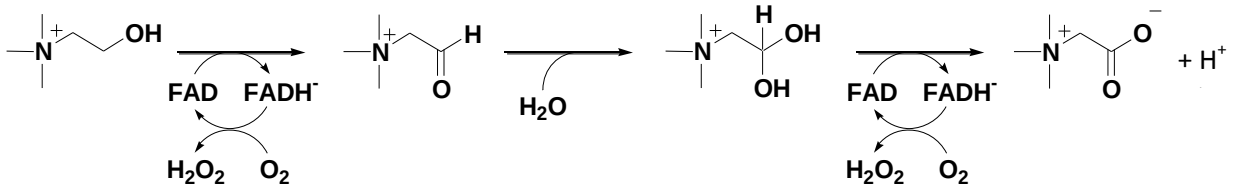

Scheme 1.1 Two step, and four electron oxidation of choline catalyzed by choline oxidase. The figure was taken from reference (*1*) without author's permission.

Choline oxidase is grouped in Glucose-Methanol-Choline (GMC) oxidoreductase superfamily, which includes choline oxidase, glucose oxidase, cholesterol oxidase, methanol oxidase, pyranose 2-oxidase and aryl-alcohol oxidase (*5*). The enzyme was first described by Ikuta at al. in 1977. This group reported the purification and earliest characterization of the enzyme from Gram-positive soil bacterium *Arthrobacter globiformis* (*6*). Thereafter, choline oxidase was also purified and characterized from *Alcaligens* sp. and *Cylindrocarpon didymium (7, 8).*To date, most of the structural and mechanistic data have accumulated from recombinant choline oxidase from *Arthrobacter globiformis*. The enzyme is significantly important in medicine and biotechnology.

1.2 Importance of Choline Oxidase

Flavin dependent enzymes are important components in biological systems. It has been estimated that ~1-3% of bacterial and eukaryotic organisms contain genes that express flavoproteins. Enzymes that contain flavin are involved in a number of biological processes including enzymatic reactions, energy metabolism, biodegradation, DNA repair, protein folding, apoptosis and neural development (*9*). Choline and glycine betaine are essential molecules in biological systems (*10, 11*). Choline is an important nutrient in humans and is required for biosynthesis and signaling functions of cellular membranes that affects lipid transfer from liver (*12*). A number of choline related enzymes were overexpressed and/or showed elevated activity in cancer. Thus, monitoring choline metabolism could be used as a diagnostic tool in cancer (*13*). Glycine betaine has been shown to be an important compound in plants and bacteria providing stability to organisms in the presence of osmotic and temperature stress without interference from the cytoplasmic reactions (*14-17*). Moreover, glycine betaine is an essential source of methyl groups for biosynthesis of methionine in the liver and kidney (*18*). In biotechnology, the

codA gene encoding choline oxidase has been used in many economically valuable plants in order to enhance the crops ability to overcome high salinity and high or low temperature stress; some examples includes, potato plants and rice crops (*19, 20*).

Choline oxidase is one of the most extensively characterized alcohol oxidizing flavin dependent enzyme. Accumulating data from choline oxidase might be applicable to related systems, such as choline dehydrogenase, a membrane associated flavin dependent enzyme (plasma membrane in bacteria and mitochondrial membrane in eukaryotic cells) (*21, 22*). The active site residues that play a role in the reaction catalyzed by choline oxidase have been shown to be fully conserved in choline dehydrogenase, suggesting that the data obtained from choline oxidase might be applicable to choline dehydrogenase.

1.3 Biophysical Properties of Choline Oxidase

Choline oxidase is a homodimer with a molecular mass of 120 kDa. Previously, mass spectroscopy, size exclusion chromatography and SDS-PAGE techniques under non denaturing conditions were used in order to determine the molecular mass and the oligomerzation state of the enzyme (*23*). The UV-visible absorbance spectrum of choline oxidase showed three maxima at 272, 373 and 454 nm, consistent with presence of FAD covalently bound to the enzyme moiety (*23*). However, the relative intensities of the peaks in the near UV and the visible regions of the absorbance spectra indicated that FAD is present as a mixture of oxidized and anionic semiquinone states (*23*). In the same study, it was shown that treating the enzyme with urea resulted in decreasing the intensity of peaks at 373 nm as well as increasing in the 454 nm peaks, consistent with fully oxidized FAD in the denatured enzyme. The UV-visible absorbance spectrum of denatured enzyme showed no difference after dialysis with decreasing amount of

urea consistent with the covalent attachment of FAD to the enzyme moiety. Furthermore, a stoichiometry of 0.88 ± 0.12 was determined for each monomer of choline oxidase containing one FAD cofactor (*23*). The results from crystallographic studies are in agreement with the solution experiments. X-ray crystal structure showed that the FAD is covalently attached to the His99 Nϵ2 atom through the FAD C8M atom of the isoalloxazine ring (*24*).

The enzyme-bound flavin was observed as a mixture of FAD_{ox}/FAD_{sq} between 35 and 85% when choline oxidase was expressed in *Escherichia coli* (*25*). It was determined that at pH 8.0, anionic semiquinone is not reactive with molecular oxygen and oxidizing agent ferricyanide (*25*). *Ab initio* theoretical calculations showed that the majority of the spin density in the anionic semiquinone localized either on the benzene ring or the N(5) position of the flavin (*25*). The N(5) atom of flavin accepts a hydride ion during the oxidation of choline, thus, it is expected to be readily accessible to molecular oxygen (*3, 25*). However, the benzene ring of flavin is covalently attached to the His99 Nϵ2 atom through a histidyl linkage (*24*) and likely it is not freely accessible to molecular oxygen due to hindrance by protein moiety (*25*). Furthermore, it was proposed that the histidyl linkage of the flavin with the protein moiety might play a role in the stabilization of the spin density on the benzene ring of the flavin through an inductive effect (*25*). The catalytic inactivity of the flavin semiquinone was also determined by UV-visible spectral analysis in which the enzyme showed catalytic cycle between fully oxidized and reduced states under turnover (*25*). These data were supported by the experiments from different preparations containing variable FAD_{ox}/FAD_{sq} ratios of enzyme, showing that the anionic semiquinone is not required for catalysis (*25*). It was suggested that a positive charge localized in close proximity to the N(1)-C(2)=O locus of the flavin in the active site of choline oxidase might stabilize the anionic semiquinone (*25*). Active site residue His466 has been determined to be

~3.3 Å away from N(1) locus of flavin (*25*). This residue was investigated via site directed mutagenesis, in order to investigate the contribution of positively charged histidine side chain in the active site of choline oxidase (*26*). A possible positive charge stabilizing the negative charge on N(1) locus in anionic semiquinone was reversed in His466Asp variant enzyme (*26*). The UV-visible absorbance spectrum of two-electron-reduced form of CHO-His466Asp at pH 6.0 indicated that the enzyme-bound flavin hydroquinone was in the neutral state (*26*). Furthermore, when the pH value was increased up to pH 10.0, no change was observed in the absorbance spectra suggesting that the negative charge of aspartyl side chain stabilizes the neutral hydroquinone in CHO-His466Asp enzyme (*26*). In contrast, it has been shown that the anionic form of hydroquinone was stabilized between pH 6.0 and 10.0 in two-electron-reduced flavin in wild type choline oxidase (*26*). A mixture of anionic and neutral hydroquinone at pH 6.0 and anionic species at pH 8.0 was observed in the CHO-His466Ala variant enzyme (*26, 27*). Accumulating data from wild type, the CHO-His466Asp and the CHO-His466Ala enzymes suggested that destabilization of the anionic semiquinone requires a negative charge in the proximity of N(1) locus of flavin (*26, 27*). It was shown that destabilization of the negative charge on the N(1) locus of reduced flavin results in removal of the covalent linkage in ~75 % of the CHO-His466Asp enzyme (*26*). Furthermore, it was concluded that a positive charge close to N(1) locus is important for the formation of covalent bond between the flavin and the protein moiety (*26*). Around 160 mV decrease in the midpoint redox potential of the enzyme bound flavin in the two electron transfer reaction was determined in CHO-His466Asp, in agreement with the importance of a positive charge close to N(1) locus of the flavin (*26*).

The redox potentials of the enzyme-bound flavin in choline oxidase have been reported to be the highest among flavoproteins, with $E_{ox/sq,7}$ = +211 mV and $E_{ox/red,7}$ =-65 mV (*26*). The study

showed that the thermodynamic stabilization of the flavin semoquinone significantly decreases when glycine betaine is bound in the active site for which the enzyme-bound flavin displays a midpoint reduction potential $E_{ox/sq,7}$ of +132 mV in choline oxidase (*26*). It was reported that the covalent attachment of flavin to the protein and a positive charge provided by His466 residue in the active site might result in perturbations in the redox potential of flavin determined by site directed mutagenesis studies (*26, 27*).

A covalent adduct formation between N(5) atom of flavin and sulfite was observed in choline oxidase (*27*). Incubating FAD_{ox} containing choline oxidase with sulfite resulted in the bleaching of the peak at 452 nm with appearance of a new peak centered at 320 nm, in agreement with adduct formation between sulfite and the N(5)-flavin atom (*27*). The enzyme showed high affinity to sulfite with a K_d value of 40 μM (at pH 7.0 and 15 ^oC), a slow rate constant was determined for the adduct formation (k_{on} = 0.04 $M^{-1}s^{-1}$), suggesting that the entrance of sulfite for the active site constrained by the negative charge locates on the sulfite molecule (*27*).

It was reported that freezing of the enzyme at pH 6.0 resulted in conformational changes that cause the enzyme to lose catalytic activity (*28*). However, the catalytic activity reverted back with a pH dependent manner when the enzyme was treated at pH ≥ 6.5 (*28*). It was concluded that the impaired ionization(s) of the protein residues are not directly accessible to the bulk solvent and associated with the conversion of the inactive and active enzyme species (*28*).

1.4 3D Structure of Choline Oxidase

The three-dimensional structure of choline oxidase from *A. globiformis* was investigated by X-ray crystallography, the crystal diffracted to a resolution of 1.8 Å (*24*). The overall crystal structure revealed that choline oxidase crystallized in the form of a homodimer with dimensions

of 88 Å x 70 Å x 46 Å consistent with results from solution experiments, gel electrophoresis and gel filtration chromatography (*23*) (Figure 1.2). It was reported that each monomer includes 546 amino acid residues (*24*). Two monomers are connected to each other with electrostatic charge complementary residues in order to form a dimer, which are Asp72-Ly398 (4.1 Å), Asp250-Glu53 (4.3 Å), Arg225-Glu370 (3.2 Å), Asp358-Arg396 (2.4 Å), Arg363-Asp394 (4.2 Å), and Arg363-Asp397 (2.9 Å) (*24*).

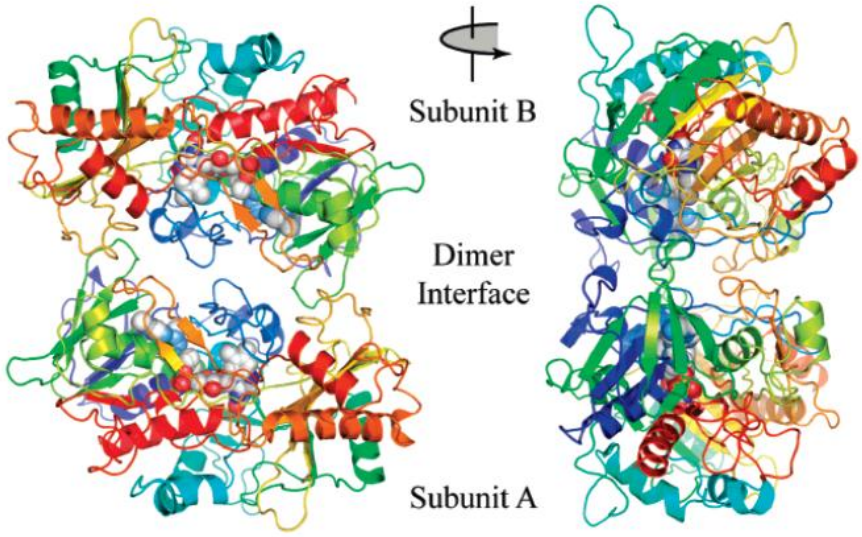

Figure 1.1. 3-D structure of choline oxidase to 1.8 Å resolution. Two orthogonal views of the enzyme illustrated with the cartoon ribbon trace of the protein backbone. The FAD is shown as CPK atoms with gray, blue and red colors representing C, N and O respectively. This figure was taken from reference (*24*) without author's permission.

The electron density maps showed that the FAD has a covalent attachment between its C8M atom and active site residue His99 Nϵ2 atom (*24*). The solvent-accessible calculations indicated that only 2.1 % of the FAD isoalloxazine ring is solvent accessible suggesting that FAD is almost completely buried within the protein (*24*). The solvent excluded active site cavity was determined with the analysis of the molecular surfaces of the enzyme with an approximate

volume of 123 $Å^3$ which is located within the substrate binding domain (*24*). The cavity is located adjacent to the *re* face of FAD and can easily accommodate the alcohol substrate (93 $Å^3$) (*24*). The cavity is partially lined by hydrophobic residues (Trp61, Trp331, Phe357, and Val464) which form an aromatic cage (*24*). The polar residues located in the cavity are His351, His466 and Glu312 which is the only negatively charged residue in the active site cavity of choline oxidase (*24*).

The interactions of active site residues with the choline substrate were analyzed by manually docking the substrate in the crystal structure of choline oxidase (Figure 1.3) (*24*). The distance between negatively charged Glu312 and positively charged trimethyammonium group of choline was measured to be 3 Å suggesting an electrostatic interaction (*24*), this is consistent with previously determined data with substrate and product inhibition studies (*29*) (see section 1.5). The model showed that positioning of the substrate is optimal for substrate activation, in which substrate hydroxyl proton abstracted by an active site base. His351 and His466 are being ~ 4 Å away from the substrate hydroxyl oxygen atom suggested that one of these residues might be serving as active site base (His466 active site catalytic base in choline oxidase, Giovanni Gadda & Crystal Smitherman, unpublished data) (*24*). Furthermore, the model revealed that the α carbon of the substrate (hydride ion donor) is less than 4 Å away from Ser101 side chain and N(5) atom of the flavin (hydride ion acceptor) (*3*, *24*).

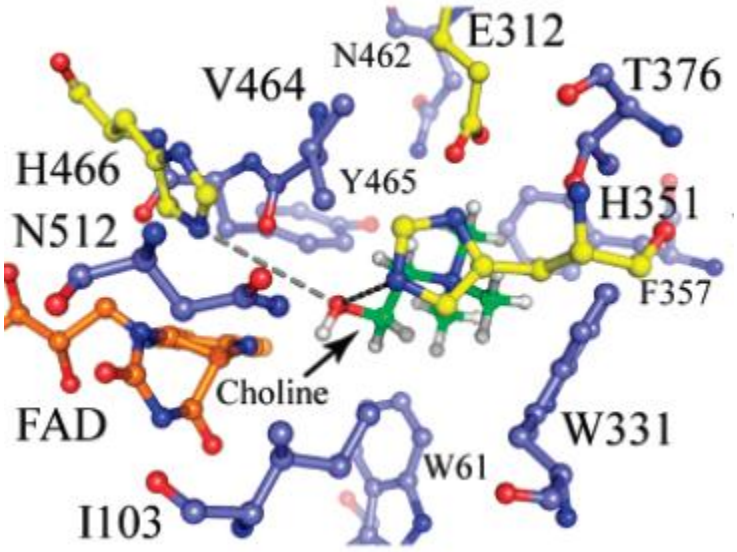

Figure 1.2. Hypothetical docking of choline molecule in the active site of choline oxidase. Blue and yellow colors represent hydrophobic and hydrophilic residues respectively. Choline is shown with green carbon atoms. The figure was taken from reference (*24*) without author's permission.

1.5 Substrate specificity and inhibitors

Steady state kinetic studies showed that choline oxidase can oxidize choline and betaine aldehyde with ${}^{app}k_{cat}$ and ${}^{app}K_m$ values of 11-15 s^{-1} and 0.6-2.3 mM under atmospheric oxygen (at pH 7.0 and 25 ^{o}C) (*23, 25*). Inhibition studies with glycine betaine indicated that the trimethylammonium group of choline is a significant determinant that defines the substrate specificity (*29*). Inhibition constants determined with glycine betaine, *N*,*N*-dimethylglycine and *N*-methylglycine decreased with each addition of methyl group on the ammonium head of the inhibitor (*29*). Furthermore, around 1 kcal mol^{-1} contribution in the binding energy by each methyl group was calculated suggesting that energetic contribution of trimethylammonium head group of choline has a significant role in the substrate binding (*29*). This conclusion was supported with steady state kinetic experiments with choline analogs (*N*,*N*-

dimethylethanolamine, *N*-methylethanolamine and 3,3-dimethyl-1-butanol) in which k_{cat}/K_m values decreased with each *N*-substituted choline analog (*29*). Moreover, it was determined that the positively charged amino head group of choline has a critical effect on the alcohol oxidation reaction in choline oxidase based on a 80-fold decrease in the k_{cat}/K_m value for oxygen upon substitution of coline with 3,3-dimethyl-1-butanol (*29*). In contrast, the inhibition constants determined with the substitution of acetate group of glycine betaine (tetramethylamine, trimethylethylamine, allyltrimethylamine and 2-amino-trimethylethylamine) showed that the acetate group of glycine betaine has no effect on the substrate binding. These data suggested that there is a thermodynamic equilibrium that makes the release of product favorable, therefore, formation of the acetate group in the alcohol oxidation reaction of choline oxidase favors product release (*29*).

Steady state kinetics and NMR studies with betaine aldehyde and its isosteric analog 3,3-dimethylbutyraldehyde showed that the hydration of betaine aldehyde is required for the second reductive half reaction catalyzed by choline oxidase, in which enzyme-bound betaine aldehyde is converted to glycine betaine (*30*). In contrast, non-hydrated 3,3-dimethylbutyraldehyde acts as a competitive inhibitor of choline oxidase with respect to choline (*30*). The study showed that betaine aldehyde oxidation occurs through a base catalyzed reaction in which a hydride ion transfers from hydrated aldehyde to the flavin (*30*). These data are consistent with choline and hydrated betaine aldehyde (*gem*-diol) having similar chemical structures with the difference of hydrated betaine aldehyde having an extra hydroxyl group on the α-carbon (*30*).

Previously, opening and closing mechanism of the active site of choline oxidase was investigated through molecular dynamics in which the substrate is directed to and the product ejected from the active site (*31*). It was proposed that a solvent accessible cluster of hydrophobic

residues, Met62, Leu65, Phe357 and Met359, works as a gate that allows the substrate to get in the active site and ejects the product (*31*). The time scale of opening and closing of the gate was determined to be10-20 ns indicating that the product release is not limiting the overall turnover of choline oxidase (*3*, *31*).

1.6 Kinetic Mechanism of Choline Oxidase

The mechanism of alcohol oxidation in choline oxidase was investigated with steady state kinetic approach by using choline and betaine aldehyde as substrates, pH profiles on substrate capture (k_{cat}/K_m) and overall turnover (k_{cat}) (*2, 4*), kinetic isotope effects by using isotopically substituted substrate and solvent, and anaerobic rapid kinetic analysis with stopped flow spectrophotometer (*3*). It was determined that the oxidation of choline to glycine betaine is limited by two chemical steps of flavin reduction (k_3 and k_7 in Fig 6.1) between pH 6.5 and 10.0 (*2, 4*).

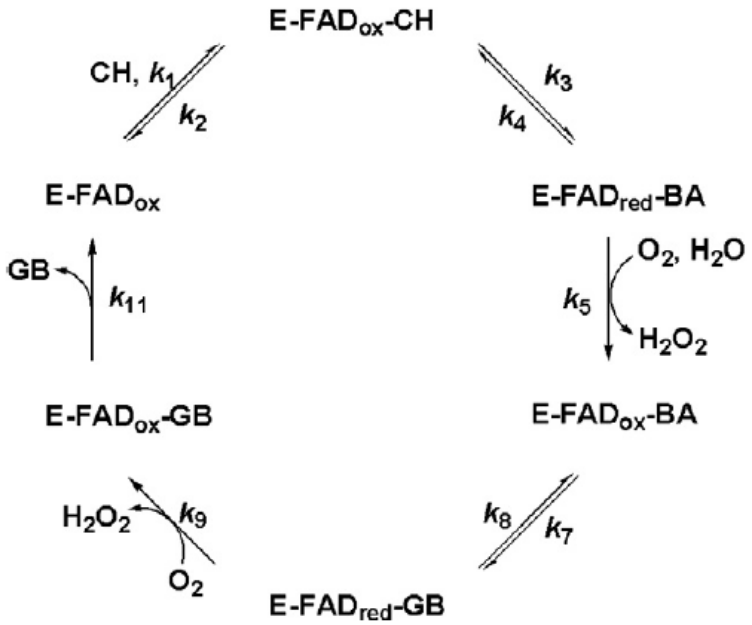

Figure 1.3. Minimal steady state kinetic mechanism of choline oxidase at pH 10. E, enzyme; FAD_{ox}, oxidized flavin; CH, choline; FAD_{red}, reduced flavin; BA, betaine aldehyde; GB, glycine betaine. The scheme was taken from reference (*32*) without author's permission.

The steady state kinetic analysis of choline oxidase with choline and betaine aldehyde as a substrate revealed that after the formation of enzyme substrate complex (E-FAD_{ox}-CH), choline is oxidized to betaine aldehyde intermediate (E-FAD_{red}-BA), the enzyme betaine aldehyde complex further reacts with molecular oxygen (first oxidative half reaction) resulting in formation of E-FAD_{ox}-BA complex and hydrogen peroxide (*2, 4*). In the second reductive half reaction flavin gets reduced by hydrated betaine aldehde forming E-FAD_{red}-GB complex. The turnover is completed by second oxidative half-reaction of flavin and product release (Scheme 1.4) (*2, 4*).

From steady state kinetic approach, the turnover number (k_{cat}) was determined as 60 s^{-1} in choline oxidase. These data are in agreement with calculated number of 55 s^{-1} for overall turnover from rapid kinetic experiments using rate constants for reduction of choline (k_3= 93 s^{-1}) and betaine aldeyhe (k_7= 135 s^{-1}), using equation 1 [See ref (*3*) for calculation]. It was concluded that the chemical steps for reduction of flavin are fully rate limiting (*3*). Independent evidence supporting this conclusion came from pH independent $^{D}k_{cat}$ values with choline and 1,2-[$^{2}H_4$]-choline (*3*). The study showed that calculated $^{D}k_{cat}$ values for choline and betaine aldehyde from rapid kinetic experiments [see ref. (*3*) for calculation] are consistent with k_{cat} being limited only by two chemical reactions (k_3 and k_7) catalyzed by choline oxidase (*3*).

$$k_{\text{cat}} = \frac{k_3 k_7}{k_3 + k_7} \qquad (1)$$

1.7 The Reductive half-reaction in choline oxidase

The alcohol oxidation reaction catalyzed in choline oxidase includes two reductive half reactions with two hydride ions transferred from choline and enzyme bound intermediate betaine aldehyde to the flavin. Reduced flavin interacts with molecular oxygen to form hydrogen peroxide. The mechanism of this reaction was previously elucidated using steady state kinetics, rapid kinetics and pH studies (*2, 3*), and by investigating various active site residues using site directed mutagenesis. Mutated residues include Ser101 (*33*), His99 (*34*), His464 (*27*), His351 (*35*), Val464 (*36*), Glu312 (*24*) and Asn510 (*37*).

The reaction catalyzed by choline oxidase was shown to be pH independent between pH values of 5.0 and 10.0 in which the substrate binding, product binding and the order of kinetic steps are not affected by pH (*2, 25*). The reductive half-reaction consists of hydroxyl proton abstraction by an active site base to activate the alcohol substrate, stabilization of the alkoxide species **,** and the hydride ion transfer from α-carbon of enzyme-alkoxide substrate to the N(5) atom of flavin (Figure 1.5) (*3*). Steady state and pH studies on k_{cat}/K_m and k_{cat} with choline as substrate indicated that a catalytic base with a pK_a value of ~7.5 accepts substrate hydroxyl proton in the activation process, furthermore, isotope effect experiments with 1,2-[$^2H_4$]-choline and inhibition studies with glycine betaine supported this conclusion (*3, 4, 25, 38*).

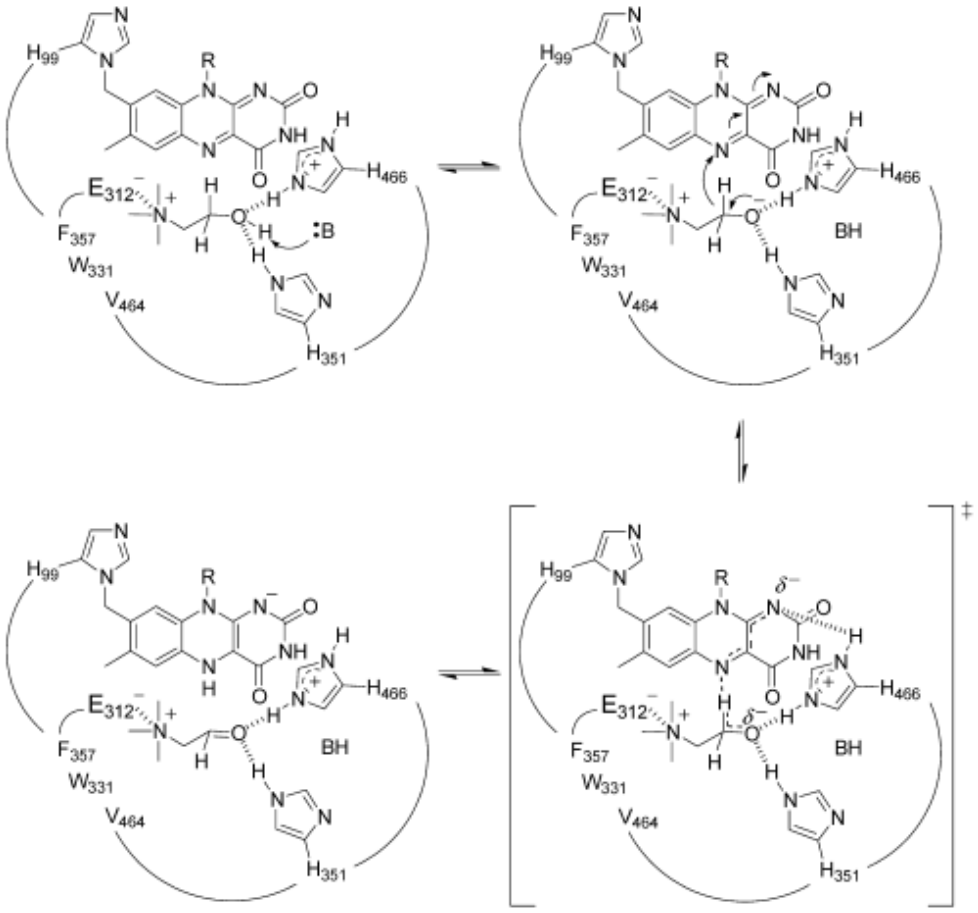

Figure 1.4. The reductive half reaction in choline oxidase. Proton abstraction by an active site base, stabilization of the alkoxide species and the hydride transfer to flavin. The figure was taken from reference (*36*) without author's permission.

Substrate and solvent deuterium isotope effect studies were used to investigate the relative timing of proton and hydride transfers (*3*). It was concluded that the choline alkoxide proton is not in flight in the same transition state as hydride transfer which indicates step wise mechanism for proton and hydride transfer in the reaction catalyzed by choline oxidase (*3*). The evidence for this conclusion came from the substrate kinetic isotope effect of ~9 when choline is substituted with 1,2-[$^{2}H_{4}$]-choline and solvent kinetic isotope effect of unity (*3*). This data ruled out the synchronous hydride transfer mechanism in which the proton and hydride are concomitantly in

flight in the same transition state (*3*). Furthermore, no significant change was observed in the substrate isotope effect on the rate of flavin reduction when aqueous solvent was substituted with deuterated solvent which indicates that the proton transfer is significantly faster than the hydride transfer (*3*). An alternative mechanism in which a single electron transferred to the flavin coupled with removal of alcohol hydroxyl proton before hydrogen transfer to the flavin from the α-carbon (Figure 1.6). This pathway was eliminated because it was expected that in such mechanism flavin radical species should be detected, however, no transient flavin radical was detected from single turnover experiments using stopped flow spectrophotometer in the reaction of flavin reduction by choline (*3*).

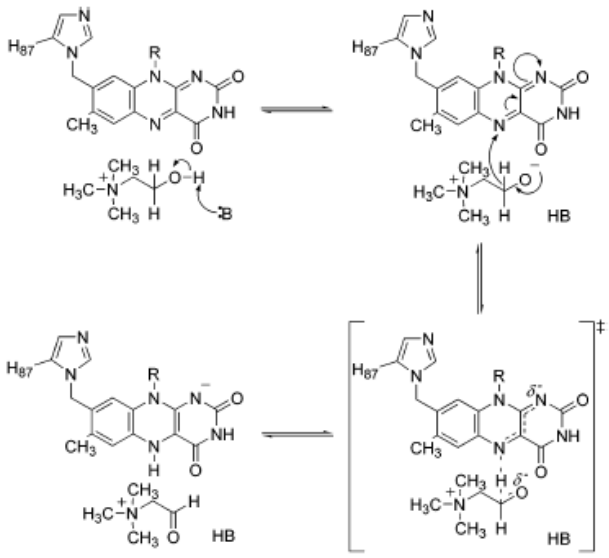

Figure 1.5. Chemical mechanism for proton and hydride ion transfer in choline oxidase. The scheme was taken from reference (*3*) without author's permission.

Stabilization of negatively charged alkoxide species for the optimal positioning of the enyme-alkoxide complex and flavin in the reductive half-reaction is achieved by electrostatic interactions and hydrogen bonding between various active site residues and the enzyme-substrate

complex. Replacement of His466 or His351 with alanine using site directed mutagenesis showed that limiting rate constants significantly (~20 fold and ~75 fold respectively) decreased in the reductive half reaction (*27, 35*). It was proposed that these residues modulate the electrophilicity of the covalently bound flavin, and provide stabilization through hydrogen bonding between imidazole side chains and the hydroxyl group of alcohol substrate (*27, 35*). Furthermore, the experimental results from S101A enzyme showed that the serine residue at 101 position also contributes to the stabilization of the enzyme-substrate complex in order to achieve optimal hydride transfer from substrate to the flavin (see section 1.10) (*33*). The negative charge of Glu312 residue has been shown to be critical in the reductive half reaction by providing an electrostatic interaction with the positively charged head group of alcohol substrate. Through this electrostatic interaction, the positioning of the substrate for optimal hydride transfer is achieved in the reductive half reaction of choline oxidase (*24*).

1.8 The oxidative half-reaction in choline oxidase

In choline oxidase each reductive half-reaction is followed by an oxidative half-reaction in which the reduced flavin is oxidized with concomitant reduction of molecular oxygen to hydrogen peroxide (Scheme 1.1) (*2-4*)

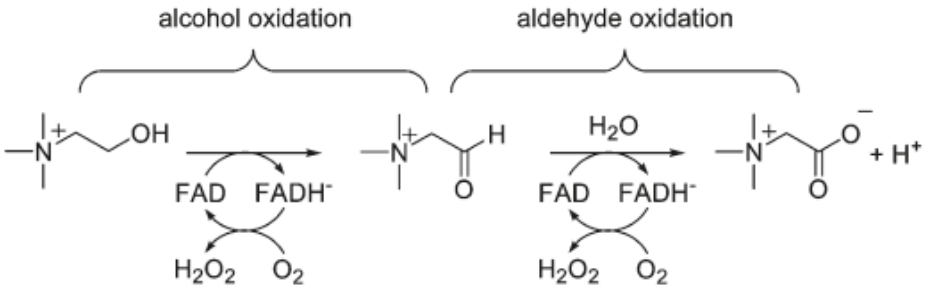

Scheme 1.2. Oxidative half reaction in choline oxidase. The figure was taken from reference (*39*) without author's permission.

A number of flavin dependent enzymes have been investigated to elucidate the activation of molecular oxygen that interacts with reduced flavin to form superoxide ($O_2^{-\bullet}$), hydrogen peroxide (H_2O_2) or water (H_2O) (*40-42*). Recent studies showed that the activation of molecular oxygen requires a positively charged group that acts as an electrostatic catalyst. It has been demonstrated that a histidine residue in glucose oxidase (*43*) and a lysine residue in sarcosine oxidase (*44*) play a significant role in the activation of molecular oxygen. Steady state kinetics with choline or a substrate analog lacking the positive charge combined with site directed mutagenesis studies demonstrated that the activation of molecular oxygen in choline oxidase is provided by a non-ionizable positively charged trimethylamine head group of the product in the alcohol oxidation reaction (Scheme 1.2) (*29, 45*). Steady state kinetics showed that k_{cat}/K_{oxygen} value decreased when 3,3-dimethybutanol lacking the positive charge used as a substrate analogue instead of choline (*29*). However, the site directed mutagenesis studies established that substitution of the three histidines with alanine (His466 and His351) and asparagine (His99) in choline oxidase resulted in ≤ 1.5 times decrease in k_{cat}/K_{oxygen} value with respect to the wild type. These data are consistent with each histidine residue not being important for the oxidative half-reaction catalyzed in choline oxidase (*29, 40*)

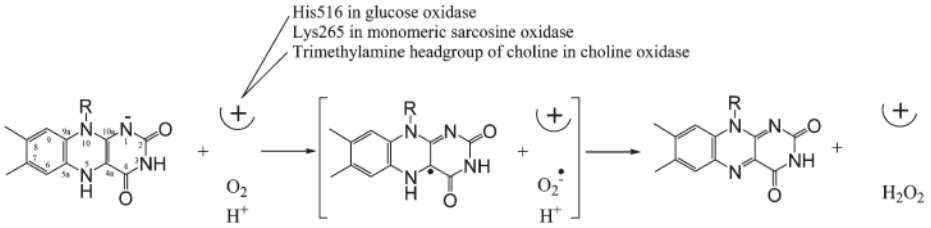

Scheme 1.3. Proposed activation mechanism of molecular oxygen in glucose oxidase, monomeric sarcosine oxidase and choline oxidase. The figure was taken from reference (*39*) without author's permission.

It was demonstrated that hydrophobic active site residue Val464 of choline oxidase plays a role in the oxidative half reaction in choline oxidase (*39*). It was concluded that the Val464 provides nonpolar site proximal to (C4a) atom of the flavin in order to navigate the molecular oxygen where it will be activated by positively charged head group of the ligand to the superoxide species (see section 1.9.5) (*39*).

1.9 Active site mutants

In choline oxidase, a number of active site residues were investigated with site directed mutagenesis approach. These data combined with x-ray crystallography, biochemical and mechanistic investigations provided useful information to understand the reaction catalyzed in choline oxidase at the molecular level.

1.9.1 His466

His466 is an active site residue that is conserved in the Glucose-Methanol-Choline (GMC) oxidoreductase superfamily (*40*). His466 position has been determined to be ~3.3 Å away from N(1) locus of flavin in choline oxidase (*25*), therefore, it was expected that this active site residue might play a role in the oxidation of the alcohol substrate. Previously, His466 was replaced with alanine and aspartate (*26, 27*). The steady state kinetics data from CHO-His466Ala enzyme showed 3-fold decrease in k_{cat}/K_m value for choline, however, no significant difference was observed in k_{cat}/K_{oxygen} value as compared to the wild type enzyme (*27*). These data indicated that His466 is involved in the reductive half reaction in which the alcohol substrate is oxidized by flavin but not in the oxidative half reaction in which reduced flavin is oxidized by molecular oxygen. Furthermore, the pH independent k_{cat}/K_{oxygen} values between pH 6.0 and 10.0 for the mutants are in agreement with His466 having no effect on the oxidative half reaction in choline

oxidase (*25*). Around 25 mV decrease in the midpoint redox potential of the enzyme-bound flavin was determined which suggested that His466 has a significant contribution to the electrophilic environment of the flavin cofactor (*27*). It was proposed that there might be a direct electrostatic interaction between Nϵ2 locus of imidazole side chain of His466 and N(1) locus of flavin (*27*). Evidence supporting such an interaction in choline oxidase came from absence of stabilization of the anionic flavin semiquinone and the sulfite N(5)-flavin adduct as seen in CHO-His466Ala (*27*). Moreover, $\Delta E_{m,7}$ value of -25mV was determined when His466 was replaced with alanine which accounts for ~4.2 kJ mol^{-1} energetic contribution in choline oxidase (*27*). This energy difference could account for 5-fold decrease in the rate of hydride transfer to the flavin (*27*). However, these data are not consistent with ~20-fold decrease in the k_{cat}/K_m values determined in CHO-His466Ala enzyme at high pH where k_{cat}/K_m value reflects the first rate limiting step in both wild type and His466Ala enzymes (*27*). In this regard, it was further suggested that His466 might also facilitate the alcohol substrate activation by stabilizing the alkoxide species in the transition state in the oxidation of choline to betaine aldehyde (*27*). Evidence supporting the presence of such stabilization came from the substrate and solvent deuterium kinetic isotope effects. It was shown that the relative timing for bond cleavage in CHO-His466Ala enzyme, hydroxyl proton cleavage is in flight in the transition state for CH bond cleavage (*27*). These data suggested that lack of transition state stabilization of alkoxide species contributed by the His466 residue would make the formation of the alkoxide species energetically unfavorable, which makes catalysis significantly slower (*27*). Independent evidence for stabilization of alkoxide species by His466 came from absence of N(5)-flavin sulfite adduct formation in CHO-His466Ala enzyme which was present in the wild type enzyme. The adduct formation was restored in the presence of exogenous imidazole in the mutant enzyme (*27*). It was

proposed that the adduct formation between N(5) flavin and the negative charge on the oxygen atom of sulfite is stabilized by the imidazole ring of His466 (*27*). Furthermore, pH profiles of the absorbance spectra of CHO-His466Ala and the wild type enzyme showed that substituting the His466 with alanine results in one unit increase of the pK_a value for the ionization of N(3) locus of flavin (*27*) consistent with decreased polarity of microenvironment of flavin N(3) locus (*46*). These data suggested that His466 modulates the polarity of the active site for efficient proton transfer from the hydroxyl group of substrate (*27*).

Choline oxidase lost enzymatic activity upon substitution of His466 with aspartate (*26*). It was concluded that reversing the positive charge near the flavin N(1) locus in choline oxidase resulted in lack of ability to stabilize negative charges in the active site irrespective of whether the negative charge is on the flavin or on the active site ligands (*26*). In this study, around 160 mV decrease in the midpoint redox potential of the enzyme bound flavin was determined when His466 was substituted with aspartate (*26*). Around 250000-fold decrease is estimated in the rate of hydride transfer to the flavin according to 160 mV decrease in the $\Delta E_{m,7}$ value for CHO-His466Asp enzyme. This further explains the complete loss of enzymatic activity (*26*).

1.9.2 His351

His351 is another active site residue that was investigated with site directed mutagenesis to understand its role in the reaction catalyzed by choline oxidase. Previously, His351 residue was substituted with alanine and it was shown that the CHO-His351Ala enzyme is properly folded with flavin covalently bound to the protein as in wild type (*35*). Anaerobic reductive-half reaction experiments with choline or betaine aldehyde in CHO-H351A enzyme showed 9 and 17 times increase in K_d values respectively (*35*). These data suggested that His351 plays an

important role in substrate binding process, likely by forming a hydrogen bond with hydroxyl oxygen of choline**.** Replacing His351 with alanine in choline oxidase resulted in increased K_d values for the substrates that correspond to 5-8 kJ mol^{-1} energy contributed by the His351 side chain. These data further supported that His351 is involved in substrate binding via hydrogen bonding interaction (*35*). X-ray crystal structure data of wild type is in agreement with His351 side chain being involved in hydrogen bonding interaction with the hydroxyl group of the alcohol substrate(s) (*35*). The crystal structures resolved to 1.8 Å where DMSO was used as an additive to mimic the substrate shows that the distance between His351 and the methyl group of DMSO is 3.5 Å (*35*). Furthermore, the N(5) atom of the flavin to where the hydride ion is transferred from the α-carbon of the alkoxide species (*3*) is 6.7 Å away from the His351. It was proposed that the His351 further facilitates the hydride transfer reaction between the alkoxide species and the N(5) atom of flavin by forming hydrogen bonds to the negatively charged oxygen atom of the alkoxide intermediate in the transition state for futher reaction (*35*). This conclusion was consistent with a 75-fold decrease in the rate constant for reduction of flavin (k_{red}) with choline as a substrate and 35- fold decrease in the k_{red} with hydrated betaine aldehyde as a substrate which were observed using rapid kinetics approach (*35*). It was previously shown that in wild type choline oxidase, the hydride transfer occurs via quantum mechanical tunneling within a highly preorganized active site where minimum independent movements are allowed between the hydride ion donor (alkoxide species) and acceptor (N(5) atom of falvin) (*38*). It was further hypothesized that the substitution of His351 with alanine could impair the preorganization of the enzyme-substrate complex by allowing increased independent movements of hydride ion donor and acceptor. Thus, the observed rate constants in the hydride transfer were decreased in CHO-His351Ala enzyme with choline and hydrated betaine aldehyde (*35*).

Furthermore, 1.2 fold lower k_{cat}/K_m value for oxygen in His351Ala enzyme reported with respect to the wild type that suggests His351 residue does not participate in the oxidation reaction of flavin by molecular oxygen (*35*).

1.9.3 His99

Active site residue His99 forms covalent bond through its Nϵ2 atom to C8M atom of flavin in choline oxidase (*24*). The contribution of covalent linkage in the oxidation reaction of alcohol substrate was investigated by replacing His99 with asparagine (*34*). The overall integrity of His99Apn variant enzyme was shown to be similar to that of the wild type enzyme through kinetic and mechanistic investigations, therefore, the mechanistic differences can be attributed to the presence or absence of His99 residue (*34*). The steady state kinetic experiments and pH studies in the CHO-His99Asn enzyme showed that an unprotonated group is required acting as a base in the reductive half-reaction, the CH bond cleavage is being the rate limiting step in the reductive half-reaction and overall turnover reaction as does wild type choline oxidase. Furthermore, no active site ionizable group was observed that is involved in the oxidative half-reaction where reduced flavin reacts with molecular oxygen (*34*).

The covalent bond between the His99 Nϵ2 atom and the CM8 atoms of flavin was shown to be play a role in the reductive half-reaction in which the alcohol substrate is oxidized to betaine aldehyde and a hydride ion is transfered to the flavin (*34*). In contrast, the covalent linkage showed no effect on the oxidative half-reaction in which molecular oxygen reacts with reduced flavin resulting in hydrogen peroxide formation (*34*). The evidence for this conclusion came from anaerobic rapid kinetic and steady state kinetic experiments. Around 45-fold decrease was observed in the limiting rate constant of anaerobic reduction of flavin (k_{red}) for CHO-His99Asn

in comparison to the wild type choline oxidase (*34*). Furthermore, steady state kinetic experiments revealed that 10-fold in k_{cat}/K_m and 30-fold decrease in k_{cat} values with respect to the wild type enzyme (*34*).

The covalent linkage between FAD and choline oxidase through His99 active site residue has been shown to be important for the optimal positioning of the substrate within the active site which is required for the environmentally enhanced tunneling of the hydride ion in reaction catalyzed by choline oxidase (*34*). It was previously determined that the hydride transfer occurs in highly preorganized active site through quantum tunneling in wild type choline oxidase (*38*). Furthermore, it was concluded that the donor and acceptor (choline-alkoxide α carbon and N(5) atom of flavin respectively) are positioned optimally for high probability of tunneling (*38*). The evidences for this conclusion came from large kinetic isotope effects on the Eyring's pre-exponential factors (A'_H/A'_D), temperature independent kinetic isotope effects, negligible energy of activation isotope effects ($\Delta E_a = (E_a)_H-(E_a)_D$) and similar enthalpy of activations ($\Delta H^{\ddagger}$) for light and heavy isotopes in wild type choline oxidase. In contrast, it was determined that the positioning of the enzyme-alkoxide complex α carbon and the N(5) atom of flavin deviates from its optimal position as a result of non-covalent attachment of flavin in CHO-His99Asn enzyme (*34*). Experimental evidences for this conclusion came from kinetic isotope effects on the Eyring's pre-exponential factors (A'_H/A'_D) value close to unity, large isotope effects on activation energies for light and heavy isotopes (ΔE_a), temperature dependent $^{D}k_{red}$ value and different enthalpy of activation energies ($\Delta H^{\ddagger}$) for protium and deuterium transfer (*34*). It was further concluded that such significant change in the CHO-His99Asn likely arises either from increased sampling of reactive configurations or misplacement of the isoalloxazine moiety of flavin with respect to the wild type choline oxidase where the hydride is transferred from the

enzyme-alkoxide complex α carbon, as a result of removal of the flavin covalent linkage in CHO-His99Asn enzyme (*34*).

1.9.4 Asn510

Asn510 in choline oxidase is another partially conserved active site residue in Glucose-Methanol-Choline (GMC) oxidoreductase enzyme super family (*37*). The role of Asn510 in the alcohol oxidation catalyzed by choline oxidase was investigated by replacing the residue with alanine, aspartate, histidine and leucine (*37*). Biophysical, mechanistic and kinetic analysis showed that these mutant enzymes maintained the overall structure with respect to the wild type enzyme (*37*). The evidences for this conclusion came from covalent attachment of flavin to the enzyme in Asn510Ala, Asn510His and Asn510Leu mutants, the sequential steady-state kinetic mechanism in Asn510Ala and Asn510His enzymes, large substrate kinetic isotope effects in the reductive half reactions of Asn510Ala and Asn510His and only minimum deviations of UV-visible absorbance spectra of all four choline oxidase variant enzymes (*37*).

The study showed that Asn510 is important for the reductive and oxidative half-reactions in the reaction catalyzed by choline oxidase, but it has a minimum involvement in the substrate binding process (*37*). The experimental results supporting these conclusions came from steady state kinetics and anaerobic rapid reaction kinetics analysis in Asn510Ala and Asn510His variant enzymes in comparison to the wild type choline oxidase (*37*). Around 600-fold decrease in ($k_{cat}/K_{choline}$) and around 30-fold decrease in the limiting rate constant for reduction of flavin (k_{red}) determined in CHO-Asn510Ala and CHO-Asn510His enzymes with respect to the wild type enzyme (*37*). Moreover, 15-fold decrease in oxidative half reaction (k_{cat}/K_{oxygen}) in Asn510His mutant and 50-fold decrease in Asn510Ala mutant in comparison to wild type indicated

involvement of Asn510 in the oxidative half-reaction in choline oxidase (*37*). It was reported that the substrate binding constant (K_d) increased by ≤ 6-fold when asparagine was substituted with all four amino acids indicating a minimum involvement of the Asn510 side chain in substrate binding reaction in the mutant enzymes (*37*).

The study showed that the chemical step of hydride transfer is the rate limiting step in overall turnover of the Asn510Ala and Asn510His enzymes as does the wild type choline oxidase (*3*, *37*). This conclusion was supported by rapid kinetics which directly measures the rate constant for hydride transfer. Calculated k_{cat} values of 0.1 s^{-1} and 3.4 s^{-1} for choline and betaine aldehyde are in agreement with the experimentally measured k_{cat} values of 0.09 s^{-1} and 3.4 s^{-1} for Asn510Ala and Asn510His enzymes respectively (*37*). Furthermore, solvent kinetic isotope effects showed that replacing Asn510 with alanine and histidine decreased the rate constant for cleavage of the substrate hydroxyl proton (*37*). It was previously determined that the substrate hydroxyl proton cleavage is faster than the CH bond cleavage as indicated by a $^{D2O}(k_{red})$ value of 0.99 in wild type enzyme (*3*). However, $^{D2O}(k_{red})$ values of 2.6 and 1.3 determined for Asn510His and Asn510Ala mutants respectively suggested that the rate constant for alcohol substrate proton cleavage is significantly decreased (*37*). Asp510 residue is located at a close proximity to His466 which is the side chain proposed to be the catalytic base in choline oxidase (unpublished data, Dr. Giovanni Gadda and Crystal Simitherman). It was suggested that decrease in the rate constants for substrate hydroxyl proton cleavage in Asn510Ala and Asn510His could arise from the disturbed orientation of His466 for optimal positioning with respect to the substrate hydroxyl group in the proton transfer reaction (*37*).

The results from multiple kinetic isotope effect experiments indicated that the relative timing of proton and hydride transfers in Asn510Ala enzyme is affected in comparison to the wild type

choline oxidase but not in Asn510His enzyme (Scheme 1.3) (*37*). The evidences supporting this conclusion came from increased solvent and substrate kinetic isotope effect in Asn510Ala enzyme which is not consistent with the stepwise mechanism of proton and hydride transfer as seen in the wild type enzyme (*37*). In contrast, decreased solvent and substrate kinetic isotope effects were calculated from multiple kinetic isotope effects experiments in Asn510His enzyme indicating that the proton and hydride transfers occur via stepwise mechanism as does wild type choline oxidase (*37*). It was proposed that the change in the relative timing in Asn510Ala enzyme could be due to the loss of a hydrogen bonding interaction between the Asn510 residue and a reaction intermediate or transition state or a close by residue that might directly interact with an intermediate species or transition state such as His466 (*27*, *37*).

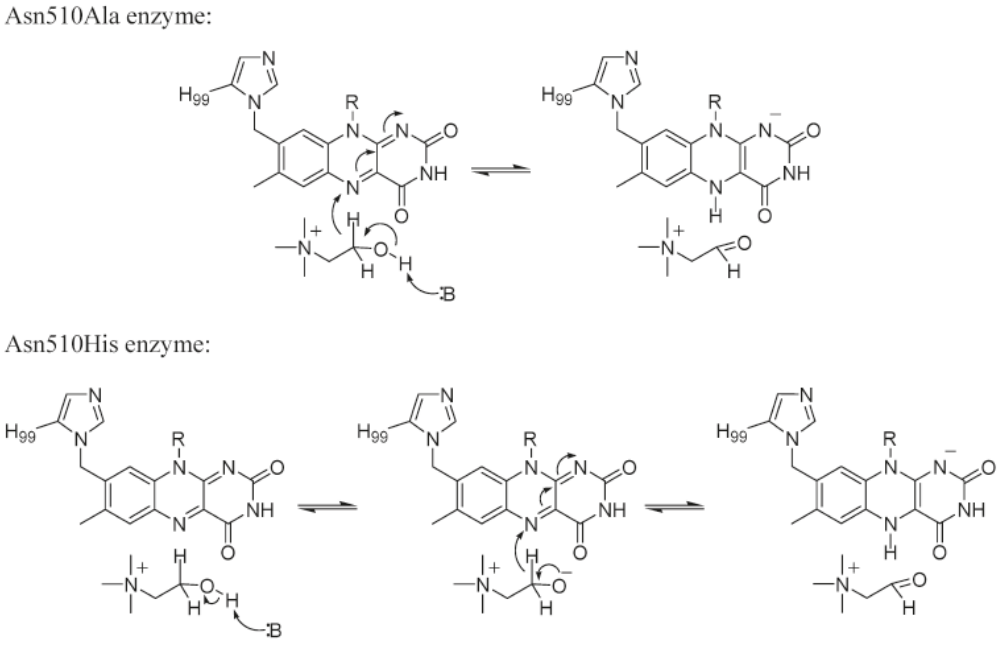

Scheme 1.4. Relative timing of proton and hydride transfers in the reactions catalyzed by Asn510Ala and Asn510His enzymes. The figure was taken from reference 12, taken without author's permission.

Asn510 also plays a role in the flavinylation reaction in which flavin is covalently attached to the His99 Nϵ2 atom through a histidyl linkage (*24, 37*). It was previously determined that the stoichiometry of covalent flavin attachment is 1:1 in wild type enzyme, however, Asn510 mutant enzymes showed 5-fold decrease in comparison to the wild type (*23, 25, 37*). It was proposed that in Asn510His, Asn510Ala and Asn510Leu enzymes, a decreased stabilization of the negative charge on the N(1)-C(2) locus of flavin which is required for the covalent attachment of flavin to the protein moiety affects the flavinylation reaction (*37*). In Asn510Asp enzyme stabilization of the negative charge on N(1)-C(2) locus of flavin was impaired to a greater extent due to negatively charged side chain of aspartate amino acid, further resulting in lack of stabilization of anionic hydroquinone which forms during the reduction of flavin reaction (*24, 37*). Such dramatic effect is in agreement with Asn510Asp enzyme being catalytically inactive (*37*).

1.9.5 Val464

Val464 is an active site residue in choline oxidase, which is located at a close proximity (~5.0Å) to the reactive center of isoalloxazine ring of flavin C(4a) and the N(5) atoms according to previously published X-ray crystal structure (*35*) (Figure 1.7) . Val464 was substituted with alanine or theronine with site directed mutagenesis in order to investigate its role in the reaction catalyzed by choline oxidase (*39*). The X-ray crystallographic data of Val464Ala showed identical structure with respect to wild type enzyme (*35*). Thus, any conclusions made from kinetic and biochemical investigations resulted from the absence of the Val464 side chain in the active site of choline oxidase (*39*). This data supported by the experimental results that showed Val464Ala enzyme shared similar properties with respect to the wild type. Such similarities include sequential steady state kinetic mechanism and pH independent k_{cat}/K_{oxygen} value with

choline (*39*). Furthermore, it was determined that Val464Ala enzyme contains covalently attached flavin to the protein moiety and stabilizes the anionic semiquinone in the presence of oxygen (*39*).

The study showed that Val464 is important for the oxidation of reduced flavin by molecular oxygen in the reaction catalyzed by choline oxidase. However, it doesn't play a role in the reductive half-reaction in which hydride ion is transfered from alkoxide-enzyme complex to the N(5) atom of flavin and the substrate binding (*39*). The substitution of valine with alanine resulted in 2-fold decrease in limiting rate constant for the reductive half reaction (k_{red}) and 5-fold decrease in the equilibrium constant for substrate binding (K_d) with respect to the wild type enzyme. In contrast, 50 fold decrease was determined in the second order rate constant value of k_{cat}/K_{oxygen} with respect to the wild type enzyme (*39*).

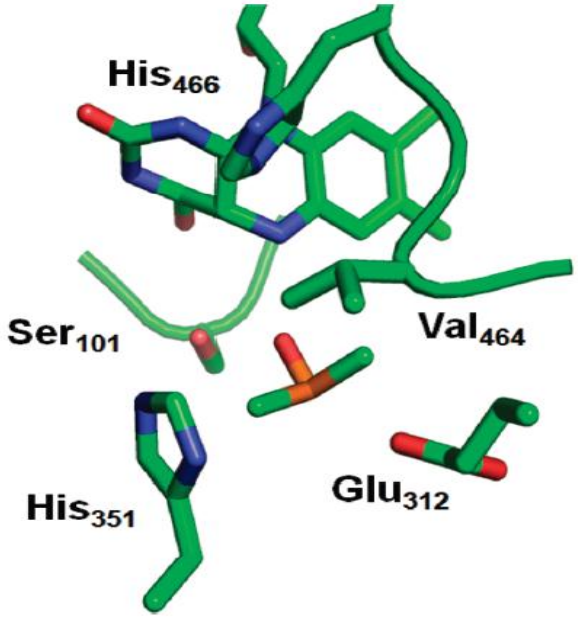

Figure 1.6. The location of Val464 at a close proximity to the flavin C(4a) and N(5). This figure was taken from reference (*35*) without author's permission.

It was proposed that the nonpolar nature of Val464 at a close proximity of C(4a) atom of flavin would attract the molecular oxygen to a site where a nearby positive charge that activates it in order to proceed the subsequent reaction with reduced flavin (*39*). The evidence for this conclusion came from a 50-fold decrease in the value of k_{cat}/K_{oxygen} indicating the involvement of Val464 in the oxidative half-reaction in which molecular oxygen interacts with reduced flavin (*39*). Moreover, the comparison of X-ray crystal structures of Val464Ala and wild type enzyme showed an increased size of a cavity which faces the C(4a)-N(5) atoms of flavin where C(4a) oxygen adduct is observed in the wild type enzyme (*39*). The study also showed that the requirement of nonpolar residue at a close proximity to the C(4a) atom is not linked to the presence of an electrostatic catalyst which activates the molecular oxygen (*39*).

1.10 Role of S101 residue and importance in catalysis

In wild type choline oxidase, Ser101 residue locates less than 4 Å away from the N(5) atom of the flavin isoalloxazine ring (*32, 33*). It was attractive to hypothesize that the hydrophilic feature of serine side chain might play a role in the reaction catalyzed by choline oxidase. Previously, Ser101 was mutated to various amino acids (Ala, Thr, Cys or Val) in order to investigate the role of this residue in the active site of choline oxidase (*32, 33*). The X-ray crystal structure of Ser101Ala was determined in a previous study with the average root-mean-square deviation (rmsd) of 0.41 Å when 527 equivalent Cα atoms compared to the wild type enzyme (Figure 1.8) (*32*). Figure 1.8 shows overlaid structure of the Ser101Ala mutant and wild type choline oxidase in which the overall structure of both enzymes are practically identical (*32*). The relative location of flavin and the active site residues were shown to be essentially no different than in the wild-type enzyme. However, an adduct formation during the crystallization process between molecular oxygen and C(4a) atom of flavin was observed in the wild type structure.

Such adduct formation was not observed in the structure of the Ser101Ala enzyme which showed a more planar flavin structure (*24*). It was hypothesized that the hydrogen bond forming ability of the serine side chain in the wild type enzyme with O(4) atom of flavin possibly stabilizes the flavin adduct formation. In contrast, such hydrogen bond forming ability is absent in Ser101Ala enzyme (*32*). Alternatively, it was suggested that lack of flavin adduct formation with molecular oxygen in the Ser101Ala enzyme could be resulting from the flavin not being reduced in the data collection process at synchrotron (*32*).

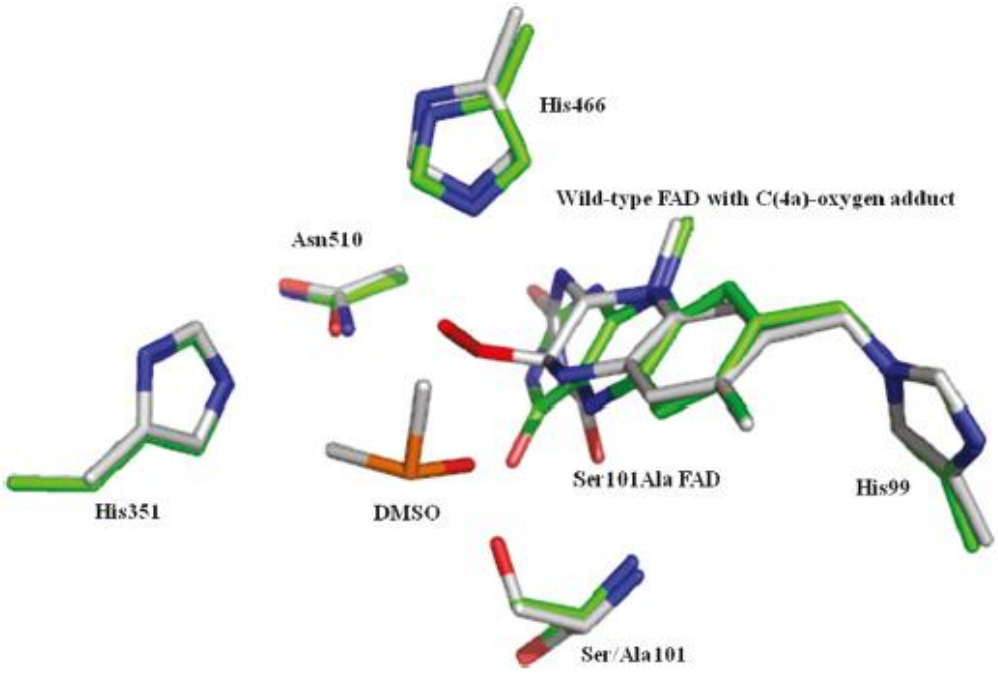

Figure 1.7. Overlaid X-ray crystal structure of wild type choline oxidase (carbons are colored gray) and S101A enzyme (carbons are colored green). The protein data bank entries are 2JBV for wild type, 3NNE for Ser101Ala mutant. The figure was taken from reference (*33*) without author's permission.

Replacement of the Ser101 residue with alanine resulted in decreased in the limiting rate constant for reductive half reaction in Ser101Ala enzyme (*32*). The results from steady-state

experiments in Ser101Ala mutant and wild type enzyme showed that a ~10 fold decrease in overall turnover (k_{cat}) and substrate capture (k_{cat}/K_m) with choline as a substrate (*32*). These data supported by the results from rapid kinetics experiments using stopped flow spectrophotometer and betaine aldehyde as a substrate showed decreased k_{red} values for flavin reduction and increased K_d values for substrate binding (*32*). Furthermore, three fold larger k_{cat}/K_{oxygen} value was determined in Ser101Ala enzyme indicating that replacement of serine side chain with alanine resulted in higher efficiency in oxidative half reaction in choline oxidase (*32*). It was proposed that substitution of Ser101 to alanine results in less hydrophilic microenvironment in the proximity of C(4a) atom of flavin which might be the reason for higher oxygen activity in mutant enzyme compared to wild type choline oxidase (*32*).

Relative timing of hydroxyl proton abstraction by an active site base and the hydride transfer from substrate to the flavin was investigated through rapid kinetics with choline for Ser101 mutants (Ser101Ala, Ser101Thr, Ser101Cys and Ser101Val) in stopped flow spectrophotometer (*33*). The results from substrate and solvent kinetic isotope effects showed that the reaction follows two well separated kinetic steps as observed in the stopped flow traces (*33*). Moreover, large kinetic solvent isotope effects of ~4 on first phase and negligible substrate kinetic isotope effect (≤ 1.1) indicated that the first phase is associated with the proton abstraction and significantly faster than the second phase (*33*). In contrast, large substrate kinetic isotope effect value of ≥ 5 on the second phase and negligible solvent kinetic isotope effects revealed that the second phase is associated with the hydride transfer and significantly slower than the first phase (*33*).

Further, it was concluded that hydroxyl group of Ser101is associated with the stabilization of the transition state for the substrate hydroxyl proton abstraction (*33*). The substitution of Ser101

with other amino acids (Ala, Thr, Cys orVal) showed that the limiting rate constants for proton abstraction is decreased by at least 15-fold in the mutant enzyme (*33*). It was proposed that the transition state for the proton transfer in wild type is stabilized by hydrogen bonding between hydroxyl group of Ser101 and the oxygen atom of alkoxide intermediate which is more electronegative than in the enzyme-substrate complex due to a negative charge on the alkoxide species (*33*). Furthermore, the hydrophilic microenvironment provided by Ser101 was shown to be associated with the hydride transfer from Cα of choline to the N(5) atom of flavin (*33*). Significant decrease in the limiting rate constants for hydride transfer was determined when S101 was substituted with less hydrophilic residues (Thr, Ala, Cys and Val) (Figure 1.9) (*33*).

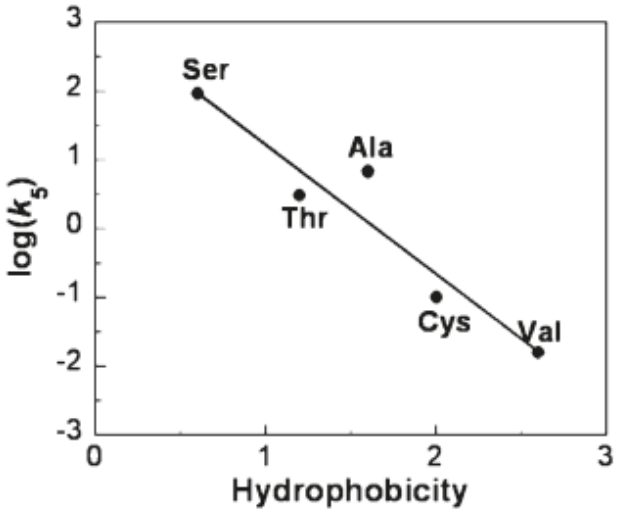

Figure 1.8. Hydrophobicity dependence of the rate constants for hydride ion transfer. The figure was taken from reference (*33*) without author's permission.

The Ser101 residue in choline oxidase is important for both activation of the substrate as well as hydride transfer reaction (*33*). A number of flavin dependent enzymes have similar catalytic strategies by having either serine, threonine or tyrosine in similar position in their active sites.

Some of the examples are class 2 dihydroorotate dehydrogenase (*47*), pyranose 2-oxidase (*48*), glucose oxidase (*49*), nitric oxide synthase (*50*), the old yellow enzyme (*51*), NADPH-cytochrome P450 oxidoreductase (*52*), alditol oxidase (*53*), UDP-galactose 4-epimerase (*54*), cholesterol oxidase (*55*), nitronate monooxygenase (*56*) and heterotetrameric sarcosine oxidase (*57*).

1.11 Quantum mechanical tunneling in wild type choline oxidase

Previously, quantum mechanical tunneling behavior of hydride transfer from α-carbon of alcohol substrate to the N(5) atom of flavin was investigated by temperature dependence of deuterium kinetic isotope effects in wild type choline oxidase (*38*). In this study, the steady state kinetics approach was used to understand the nature of hydride ion transfer by investigating the overall turnover (k_{cat}) and substrate capture (k_{cat}/K_m) with choline (*38*).

These experiments were conducted at high pH as it was determined that the reaction catalyzed by choline oxidase is pH independent at alkaline pH values (*38*). The pH profiles of $^{D}(k_{cat}/K_m)$ and $^{D}(k_{cat})$ values determined with choline and 1,2-[$^{2}H_4$]-choline as substrates showed pH independent behavior in which the hydride transfer is not being masked by any other kinetic step (*3*). Furthermore, the effect of oxygen availability on the kinetic isotope effects was investigated in order to probe the reversibility of the hydride transfer at different oxygen concentrations (*38*). The reversibility of the hydride transfer is affected by the oxygen availability in which the forward partition of the betaine aldehyde-enzyme complex during the reaction is significantly higher than reverting back to the oxidized enzyme-alkoxide complex in presence of high oxygen concentration ($\geq$ 0.97 mM) at hight pH (*38*). The study showed that at saturating oxygen concentrations and at high pH in steady state kinetic experiments the calculated kinetic isotope

effects for the hydride ion transfer catalyzed in choline oxidase approaches the value of intrinsic kinetic isotope effects (*3, 38*).

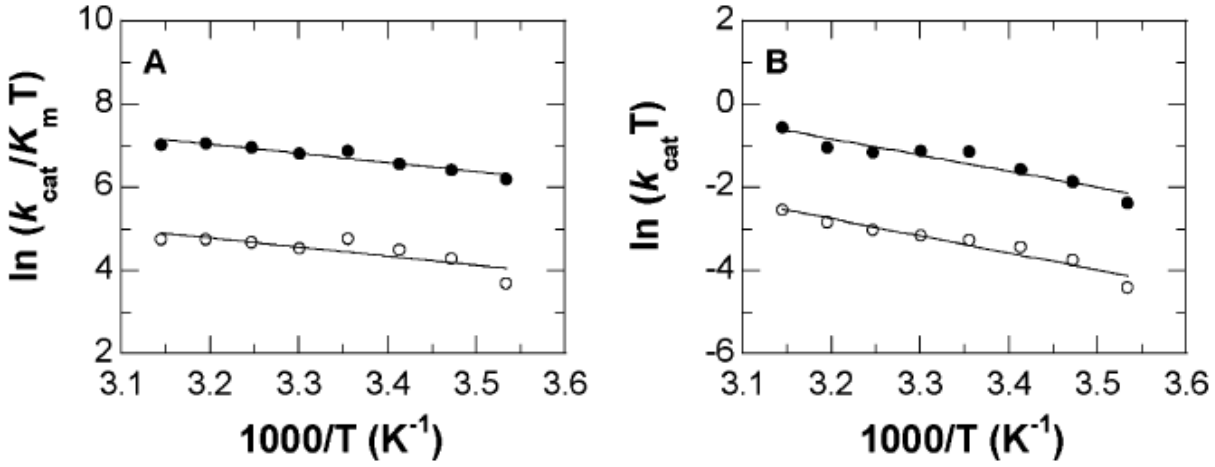

Figure 1.9. Temperature dependence of k_{cat}/K_m (Panel A) and k_{cat} (Panel B). Black circles represent choline and white circles represent 1,2-[$^2H_4$]-choline. This figure was taken from reference (*38*) without author's permission.

It was determined that the hydride ion transfer in choline oxidase from α-carbon of choline to the N(5) of flavin occurs via quantum mechanical tunneling rather than over the barrier within highly preorganized active site (*38*). In this study the temperature effects on the $^D(k_{cat}/K_m)$ and $^D(k_{cat})$ values were determined at saturating oxygen concentrations and within pH independent region in order to analyze the quantum behavior of hydride ion transfer (*38*). The Eyring's analysis was used to determine the temperature dependence of k_{cat}/K_m and k_{cat} values (Figure 1.10). A value of ~14 for isotope effects on Arrhenius prefactors (A_H'/A_D') for k_{cat}/K_m was calculated from the Eyring's plots (determined from the ratio of the y-intercepts) (*38*). It was proposed that such large isotope effects on A_H'/A_D' might be used as a evidence for ruling out classical over the barrier behavior for hydride transfer for which between 0.7 and 1.7 were predicted to be the range for classical behavior (*38, 58*). Furthermore, temperature independent

$^{D}(k_{cat}/K_m)$ values (Figure 1.11) and similar enthalpy of activations for CH and CD bond cleavages (~18 kJ mol^{-1}) in the reductive half reaction (k_{cat}/K_m) from Eyring's analysis are consistent with environmentally enhanced tunneling behavior in the hydride transfer reaction of choline oxidase (*38, 59*). Temperature independent kinetic isotope effects on k_{cat}/K_m are in agreement with the enzyme-substrate complex forms in the preorganized active site in which minimum deviation of the tunneling probability effected by the environmental influences of the reaction coordinate other than affecting the distance between donor and acceptor in choline oxidase (*38*).

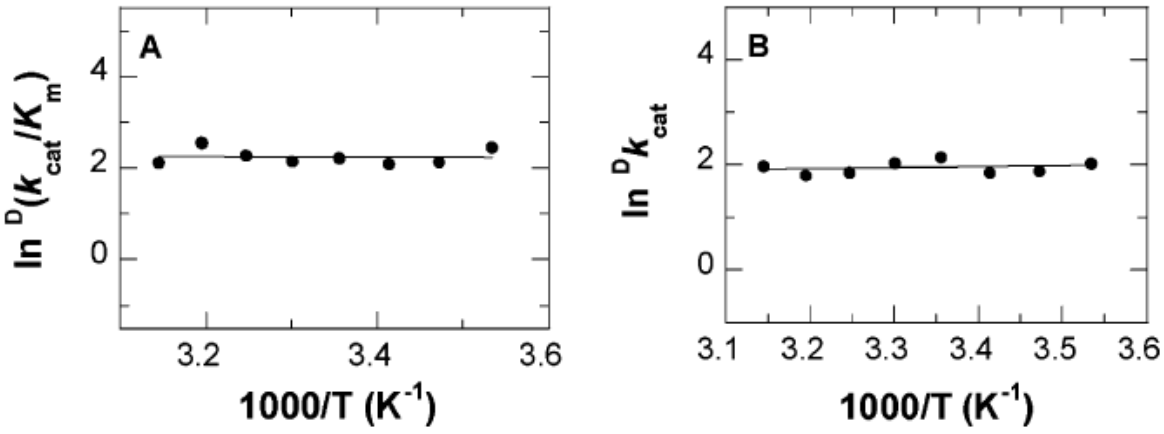

Figure 1.10. Temperature dependence of $^{D}(k_{cat}/K_m)$ and $^{D}(k_{cat})$ values with choline and 1,2-[$^{2}H_4$]-choline as substrates. The figure was taken from reference (*38*) without author's permission.

In that study, k_{cat}/K_m value was used to make all the conclusions which directly probe the first chemical step in oxidation of choline to betaine aldehyde. In contrast, the k_{cat} value includes two chemical steps, oxidation of choline and oxidation of betaine aldehyde. The author's avoided making mechanistic interpretations from k_{cat} values, however, the temperature dependency of

$^{D}k_{cat}$ and k_{cat} values calculated qualitatively very similar to those calculated for $^{D}(k_{cat}/K_{m})$ and k_{cat}/K_{m} values which is consistent with the conclusions drawn for the first chemical step (*38*).

1.12 Specific Goals

This thesis aims to investigate the quantum mechanical tunneling of the proton and hydride transfers of the choline oxidase S101A variant enzyme. The contribution of the hydrophilic active side residue Ser101 in the alcohol oxidation reaction of choline oxidase will be investigated in CHO-S101A variant enzyme by temperature dependence on kinetic isotope effects in the proton and hydride transfer reaction using stopped flow rapid kinetics approach. Biochemical and mechanistic investigations of wild type and various mutants of choline oxidase have been of great interest for medicine and biotechnology. Up to date, the transition state theory is the most acceptable theory that provides insight in the catalytic power of enzymes, however, accumulating body of data in many enzymes including choline oxidase pointed out that coupling of environmental vibrations in the microenvironment could play a significant role in enzymatic reactions as well as the quantum behavior of the particles such as proton (H^{+}), hydrogen atom (H), or hydride ion (H^{-}). It is attractive to hypothesize that the biophysical properties of molecules and enzymes could be used to diagnose and cure diseases which related to an impaired enzymatic reaction. This study has a great contribution to current investigations of quantum behavior of particles in enzymatic reactions.

1.13 References

1. Gadda, G. (2008) Hydride transfer made easy in the reaction of alcohol oxidation catalyzed by flavin-dependent oxidases, *Biochemistry 47*, 13745-13753.
2. Gadda, G. (2003) Kinetic mechanism of choline oxidase from *A. globiformis*, *Biochimica et biophysica acta 1646*, 112-118.
3. Fan, F., and Gadda, G. (2005) On the catalytic mechanism of choline oxidase, *J. Am.Chem. Soc. 127*, 2067-2074.
4. Gadda, G. (2003) pH and deuterium kinetic isotope effects studies on the oxidation of choline to betaine-aldehyde catalyzed by choline oxidase, *Biochimica et biophysica acta 1650*, 4-9.
5. Cavener, D. R. (1992) GMC oxidoreductases. A newly defined family of homologous proteins with diverse catalytic activities, *J Mol Biol 223*, 811-814.
6. Ikuta, S., Imamura, S., Misaki, H., and Horiuti, Y. (1977) Purification and characterization of choline oxidase from Arthrobacter globiformis, *J Biochem 82*, 1741-1749.
7. Ohta-Fukuyama, M., Miyake, Y., Emi, S., and Yamano, T. (1980) Identification and properties of the prosthetic group of choline oxidase from Alcaligenes sp, *J Biochem 88*, 197-203.
8. Yamada, H., Cohen, R. E., and Ballou, C. E. (1979) Characterization of 3-O-methyl-D-mannose polysaccharide precursors in Mycobacterium smegmatis, *The Journal of biological chemistry 254*, 1972-1979.
9. Kodali, V. K., and Thorpe, C. (2010) Oxidative protein folding and the Quiescin-sulfhydryl oxidase family of flavoproteins, *Antioxid Redox Signal 13*, 1217-1230.

10. Ueland, P. M. (2011) Choline and betaine in health and disease, *J Inherit Metab Dis 34*, 3-15.

11. Lever, M., and Slow, S. (2010) The clinical significance of betaine, an osmolyte with a key role in methyl group metabolism, *Clin Biochem 43*, 732-744.

12. Zeisel, S. H., and Blusztajn, J. K. (1994) Choline and human nutrition, *Annu Rev Nutr 14*, 269-296.

13. Glunde, K., Bhujwalla, Z. M., and Ronen, S. M. (2011) Choline metabolism in malignant transformation, *Nat Rev Cancer 11*, 835-848.

14. Vilhelmsson, O., and Miller, K. J. (2002) Humectant permeability influences growth and compatible solute uptake by Staphylococcus aureus subjected to osmotic stress, *J Food Prot 65*, 1008-1015.

15. Peddie, B. A., Wong-She, J., Randall, K., Lever, M., and Chambers, S. T. (1998) Osmoprotective properties and accumulation of betaine analogues by Staphylococcus aureus, *FEMS Microbiol Lett 160*, 25-30.

16. Peddie, B. A., Chambers, S. T., and Lever, M. (1996) Is the ability of urinary tract pathogens to accumulate glycine betaine a factor in the virulence of pathogenic strains?, *J Lab Clin Med 128*, 417-422.

17. Sakamoto, A., Alia, and Murata, N. (1998) Metabolic engineering of rice leading to biosynthesis of glycinebetaine and tolerance to salt and cold, *Plant Mol Biol 38*, 1011-1019.

18. Pajares, M. A., and Perez-Sala, D. (2006) Betaine homocysteine S-methyltransferase: just a regulator of homocysteine metabolism?, *Cell Mol Life Sci 63*, 2792-2803.

19. Sakamoto, A., Valverde, R., Alia, Chen, T. H., and Murata, N. (2000) Transformation of Arabidopsis with the codA gene for choline oxidase enhances freezing tolerance of plants, *Plant J 22*, 449-453.

20. Alia, Kondo, Y., Sakamoto, A., Nonaka, H., Hayashi, H., Saradhi, P. P., Chen, T. H., and Murata, N. (1999) Enhanced tolerance to light stress of transgenic Arabidopsis plants that express the codA gene for a bacterial choline oxidase, *Plant Mol Biol 40*, 279-288.

21. Rendina, G., and Singer, T. P. (1959) Studies on choline dehydrogenase. I. Extraction in soluble form, assay, and some properties of the enzyme, *The Journal of biological chemistry 234*, 1605-1610.

22. Russell, R., and Scopes, R. K. (1994) Use of hydrophobic chromatography for purification of the membrane-located choline dehydrogenase from a Pseudomonas strain, *Bioseparation 4*, 279-284.

23. Fan, F., Ghanem, M., and Gadda, G. (2004) Cloning, sequence analysis, and purification of choline oxidase from Arthrobacter globiformis: a bacterial enzyme involved in osmotic stress tolerance, *Archives of biochemistry and biophysics 421*, 149-158.

24. Quaye, O., Lountos, G. T., Fan, F., Orville, A. M., and Gadda, G. (2008) Role of Glu312 in binding and positioning of the substrate for the hydride transfer reaction in choline oxidase, *Biochemistry 47*, 243-256.

25. Ghanem, M., Fan, F., Francis, K., and Gadda, G. (2003) Spectroscopic and kinetic properties of recombinant choline oxidase from Arthrobacter globiformis, *Biochemistry 42*, 15179-15188.

26. Ghanem, M., and Gadda, G. (2006) Effects of reversing the protein positive charge in the proximity of the flavin N(1) locus of choline oxidase, *Biochemistry 45*, 3437-3447.

27. Ghanem, M., and Gadda, G. (2005) On the catalytic role of the conserved active site residue His466 of choline oxidase, *Biochemistry 44*, 893-904.

28. Hoang, J. V., and Gadda, G. (2007) Trapping choline oxidase in a nonfunctional conformation by freezing at low pH, *Proteins 66*, 611-620.

29. Gadda, G., Powell, N. L., and Menon, P. (2004) The trimethylammonium headgroup of choline is a major determinant for substrate binding and specificity in choline oxidase, *Archives of biochemistry and biophysics 430*, 264-273.

30. Fan, F., Germann, M. W., and Gadda, G. (2006) Mechanistic studies of choline oxidase with betaine aldehyde and its isosteric analogue 3,3-dimethylbutyraldehyde, *Biochemistry 45*, 1979-1986.

31. Xin, Y., Gadda, G., and Hamelberg, D. (2009) The cluster of hydrophobic residues controls the entrance to the active site of choline oxidase, *Biochemistry 48*, 9599-9605.

32. Finnegan, S., Yuan, H., Wang, Y. F., Orville, A. M., Weber, I. T., and Gadda, G. (2010) Structural and kinetic studies on the Ser101Ala variant of choline oxidase: catalysis by compromise, *Archives of biochemistry and biophysics 501*, 207-213.

33. Yuan, H., and Gadda, G. (2011) Importance of a serine proximal to the C(4a) and N(5) flavin atoms for hydride transfer in choline oxidase, *Biochemistry 50*, 770-779.

34. Quaye, O., Cowins, S., and Gadda, G. (2009) Contribution of flavin covalent linkage with histidine 99 to the reaction catalyzed by choline oxidase, *The Journal of biological chemistry 284*, 16990-16997.

35. Rungsrisuriyachai, K., and Gadda, G. (2008) On the role of histidine 351 in the reaction of alcohol oxidation catalyzed by choline oxidase, *Biochemistry 47*, 6762-6769.

36. Finnegan, S., and Gadda, G. (2008) Substitution of an active site valine uncovers a kinetically slow equilibrium between competent and incompetent forms of choline oxidase, *Biochemistry 47*, 13850-13861.

37. Rungsrisuriyachai, K., and Gadda, G. (2010) Role of asparagine 510 in the relative timing of substrate bond cleavages in the reaction catalyzed by choline oxidase, *Biochemistry 49*, 2483-2490.

38. Fan, F., and Gadda, G. (2005) Oxygen- and temperature-dependent kinetic isotope effects in choline oxidase: correlating reversible hydride transfer with environmentally enhanced tunneling, *Journal of the American Chemical Society 127*, 17954-17961.

39. Finnegan, S., Agniswamy, J., Weber, I. T., and Gadda, G. (2010) Role of valine 464 in the flavin oxidation reaction catalyzed by choline oxidase, *Biochemistry 49*, 2952-2961.

40. Gadda, G. (2012) Oxygen activation in flavoprotein oxidases: the importance of being positive, *Biochemistry 51*, 2662-2669.

41. Klinman, J. P. (2007) How do enzymes activate oxygen without inactivating themselves?, *Acc Chem Res 40*, 325-333.

42. Massey, V. (1994) Activation of molecular oxygen by flavins and flavoproteins, *The Journal of biological chemistry 269*, 22459-22462.

43. Roth, J. P., Wincek, R., Nodet, G., Edmondson, D. E., McIntire, W. S., and Klinman, J. P. (2004) Oxygen isotope effects on electron transfer to O2 probed using chemically modified flavins bound to glucose oxidase, *Journal of the American Chemical Society 126*, 15120-15131.

44. Zhao, G., Bruckner, R. C., and Jorns, M. S. (2008) Identification of the oxygen activation site in monomeric sarcosine oxidase: role of Lys265 in catalysis, *Biochemistry 47*, 9124-9135.

45. Gadda, G., Fan, F., and Hoang, J. V. (2006) On the contribution of the positively charged headgroup of choline to substrate binding and catalysis in the reaction catalyzed by choline oxidase, *Archives of biochemistry and biophysics 451*, 182-187.

46. Massey, V., and Ganther, H. (1965) On the interpretation of the absorption spectra of flavoproteins with special reference to D-amino acid oxidase, *Biochemistry 4*, 1161-1173.

47. Kow, R. L., Whicher, J. R., McDonald, C. A., Palfey, B. A., and Fagan, R. L. (2009) Disruption of the proton relay network in the class 2 dihydroorotate dehydrogenase from Escherichia coli, *Biochemistry 48*, 9801-9809.

48. Pitsawong, W., Sucharitakul, J., Prongjit, M., Tan, T. C., Spadiut, O., Haltrich, D., Divne, C., and Chaiyen, P. (2010) A conserved active-site threonine is important for both sugar and flavin oxidations of pyranose 2-oxidase, *The Journal of biological chemistry 285*, 9697-9705.

49. Wohlfahrt, G., Witt, S., Hendle, J., Schomburg, D., Kalisz, H. M., and Hecht, H. J. (1999) 1.8 and 1.9 A resolution structures of the Penicillium amagasakiense and Aspergillus niger glucose oxidases as a basis for modelling substrate complexes, *Acta Crystallogr D Biol Crystallogr 55*, 969-977.

50. Panda, S. P., Gao, Y. T., Roman, L. J., Martasek, P., Salerno, J. C., and Masters, B. S. (2006) The role of a conserved serine residue within hydrogen bonding distance of FAD in redox properties and the modulation of catalysis by Ca2+/calmodulin of constitutive nitric-oxide synthases, *The Journal of biological chemistry 281*, 34246-34257.

51. Xu, D., Kohli, R. M., and Massey, V. (1999) The role of threonine 37 in flavin reactivity of the old yellow enzyme, *Proceedings of the National Academy of Sciences of the United States of America 96*, 3556-3561.

52. Shen, A. L., and Kasper, C. B. (1996) Role of Ser457 of NADPH-cytochrome P450 oxidoreductase in catalysis and control of FAD oxidation-reduction potential, *Biochemistry 35*, 9451-9459.

53. Forneris, F., Heuts, D. P., Delvecchio, M., Rovida, S., Fraaije, M. W., and Mattevi, A. (2008) Structural analysis of the catalytic mechanism and stereoselectivity in Streptomyces coelicolor alditol oxidase, *Biochemistry 47*, 978-985.

54. Liu, Y., Thoden, J. B., Kim, J., Berger, E., Gulick, A. M., Ruzicka, F. J., Holden, H. M., and Frey, P. A. (1997) Mechanistic roles of tyrosine 149 and serine 124 in UDP-galactose 4-epimerase from Escherichia coli, *Biochemistry 36*, 10675-10684.

55. Lyubimov, A. Y., Lario, P. I., Moustafa, I., and Vrielink, A. (2006) Atomic resolution crystallography reveals how changes in pH shape the protein microenvironment, *Nature chemical biology 2*, 259-264.

56. Ha, J. Y., Min, J. Y., Lee, S. K., Kim, H. S., Kim do, J., Kim, K. H., Lee, H. H., Kim, H. K., Yoon, H. J., and Suh, S. W. (2006) Crystal structure of 2-nitropropane dioxygenase complexed with FMN and substrate. Identification of the catalytic base, *The Journal of biological chemistry 281*, 18660-18667.

57. Chen, Z. W., Hassan-Abdulah, A., Zhao, G., Jorns, M. S., and Mathews, F. S. (2006) Heterotetrameric sarcosine oxidase: structure of a diflavin metalloenzyme at 1.85 A resolution, *J Mol Biol 360*, 1000-1018.

58. Bell, R. P. (**1974**) In *Chem. Soc. Rev.*

59. Knapp, M. J., and Klinman, J. P. (2002) Environmentally coupled hydrogen tunneling. Linking catalysis to dynamics, *European journal of biochemistry / FEBS 269*, 3113-3121.

CHAPTER 2.

PROTON and HYDRIDE TRANSFER in CHO-S101A

2.1 Introduction

Understanding how enzymes catalyze reactions has been a great interest for scientist because enzymes can accelerate biochemical reaction by factors as high as 10^{20} with eminent selectivity and they are involved in many biological systems, medicine and biotechnology . Proton (H^+), hydrogen atom (H), or hydride ion (H^-) transfers are present in variety of enzymes that have been investigated to understand the catalytic power of enzymes (*1*) . To date, a growing amount of data from experimental and computational studies revealed that hydrogen transfer takes place via quantum mechanical tunneling (*1-6*). It has been hypothesized that coupling of protein dynamics from millisecond to femtosecond time scale might influence hydrogen tunneling mechanisms (*1, 2, 7, 8*). Hydrogen atom has a unique feature that is distinguished from heavier atoms in biological reactions by having very small mass, therefore, it is attractive to investigate the quantum mechanical behavior of dynamics of hydrogen chemistry (*1, 9*). The wave particle duality states that each particle has a wavelength associated to its mass at a fixed energy. The quantum mechanical behavior heavily depends on the wavelength of the particle and the distance traveled between the donor and acceptor (*1, 10, 11*). Therefore, small changes in donor-acceptor distance could affect the hydrogen tunneling behavior. A number of enzymes have been scrutinized in recent years including soybean lypoxygenase-1 (*12, 13*), alcohol dehyrogenses (*3*), dihyrofolate reductase (*14, 15*), morphinone reductase (*11, 16*), glucose oxidase (*1, 17*) and choline oxidase (*10*) in order to elucidate tunneling mechanism.

In recent years, the catalytic mechanism of choline oxidase has been extensively studied, choline oxidase catalyze the four-electron oxidation of choline to glycine betaine with betaine

aldehyde as an intermediate, FAD is reduced by the alcohol substrate and oxidized by molecular oxygen to give hydrogen peroxide (Sheme 2.1) (*10, 18-31*). Previous studies have revealed the mechanistic details of deprotonation of the hydroxyl group of the alcohol substrate by an active site catalytic base (His466, Giovanni Gadda & Crystal Smitherman, unpublished data) that yields a negatively charged alkoxide species (*18, 19*). Further in the reaction, through electrostatic interactions and hydrogen bonds with a number of active site residues, the alkoxide species positions optimally for the hydride transfer from the α-carbon of the substrate to the flavin N(5) atom. In wild-type choline oxidase, the temperature dependence of KIEs with steady-state approach was used to elucidate the hydride transfer mechanism. It has been shown that the hydride transfer in wild-type enzyme occurs via quantum mechanical tunneling within a highly preorganized active site, suggested by similar enthalpies of activations values of ~18 kJ mol^{-1} for CH and CD bond cleavage, a ΔE_a value close to unity and inflated isotope effects on Eyring's prefactors (A_H'/A_D') (*10*).

The X-ray crystal structure studies revealed that Ser101 located less than 4 Å from the flavin N(5) atom (Figure 2.1) (*32*). Hydrophilic nature of Ser101 position has been shown to be required for the proton and hydride transfer in a stepwise mechanism through stabilizing the negatively charged alkoxide intermediate via hydrogen bonding (*31, 32*). Relative timing of hydroxyl proton abstraction by an active site base and the hydride transfer from substrate to the flavin was investigated through rapid kinetics for the CHO-S101A enzyme. Substrate and solvent kinetic isotope effects showed that the reaction follows two well separated kinetic steps as observed in the stopped flow traces (*31*). Moreover, large kinetic solvent isotope effects of ~4 on first phase and negligible substrate kinetic isotope effect (≤ 1.1) indicated that the first phase is associated with the proton abstraction and significantly faster than the second phase. In

contrast, large substrate kinetic isotope effect value of ≥ 5 on the second phase and negligible solvent kinetic isotope effects revealed that the second phase is associated with the hydride transfer and significantly slower than the first phase (*31*).

In this study, the CHO-S101A variant enzyme was prepared to determine the temperature dependence of limiting rate constants for proton and hydride transfer with stopped-flow rapid kinetic approach. The contribution of the hydroxyl group of Ser101 toward the quantum mechanical tunneling of the proton and hydride transfer were investigated.

2.2 Experimental Procedures

Materials. Choline chloride was from ICN (Aurora, OH). 1,2-[$^2H_4$]-Choline bromide was from Isotech INC. (Miamisburg, OH). Glucose and glucose oxidase were from Sigma-Aldrich (St. Louis, MO). All other reagents used were of the highest purity commercially available.

Instruments. Stopped-flow experiments were conducted using a Hi-Tech SF-61 double-mixing stopped-flow spectrophotometer.

Expression and Purification of Ser101 mutant enzyme. The gene coding for the CHO-S101 enzyme variant was expressed by using the plasmid pET/*codA* S101A in *Escherichia coli* strain Rosetta(DE3)pLysS. The mutant enzyme is expressed and purified by using the same protocol previously used for the wild type enzyme (8). In order to obtain oxidized and active mutant enzyme, the enzyme solutions were dialyzed at pH 6.0 and the oxidization of flavin was monitored by spectrophotometric analysis. The enzyme was stored in 20 mM Tris-Cl pH 8.0 buffer.

Rapid Kinetic Assays. In this experiment the choline oxidase Ser101Ala enzyme solution was loaded on a tonometer and 25 cycles of degassing were applied by alternating vacuum and flushing process with oxygen-free argon (pretreated with an oxygen scrubbing cartridge, Agilent,

Palo Alto, CA). The procedure continued with mounting the degassed enzyme solution onto the stopped-flow instrument, which had been treated with an oxygen removing system including of 2 mM glucose and 0.5 µM glucose oxidase. The observed rate constants for flavin reduction of the enzyme were determined by mixing various concentrations of the substrate (choline or 1,2-[$^2H_4$]-choline) and the enzyme anaerobically in the stopped-flow spectrophotometer in 50 mM sodium pyrophosphate (pH 10.0) at 15-37 ^oC, as previously described (5). The enzyme and the substrate were mixed in equal amounts in the presence of glucose (2 mM)/glucose oxidase (0.5 μM) mixture, yielding enzyme concentration of ~10 μM. Substrate concentrations were $\geq$ 40 μM to obtain pseudo-first-order conditions. The data was collected from photomultiplier at 450 nm in dual beam mode. In solvent kinetic isotope effect experiments, the first order rate constants for flavin reduction were determined by using either 99.9% deuterium oxide or water in preparation for the buffer, substrates and the enzyme. The pD values were determined by addition of 0.4 to the pH electrode readings and adjusted with NaOD.

Steady-State Kinetic Assays

Enzyme activity was monitored by measuring the initial rates of oxygen consumption with a Hansatech oxygen electrode thermostated at 15 ^oC or 37 ^oC. The assays were carried out in 50 mM sodium pyrophosphate at pH 10.0. The steady state kinetic parameters were determined by varying the concentration of choline and 1,2-[$^2H_4$]-choline from 0.05 mM to 6 mM at fixed concentrations of oxygen from 0.06 mM to 0.135 mM. The reactions were started by adding choline oxidase into the reaction mixture with final concentration of 0.1-0.6 µM and 1 mL final volume. The reaction mixtures were equilibrated with fixed oxygen concentrations by bubbling O_2/N_2 gas mixture for at least 5 min. Substrate KIEs were determined by alternating choline and 1,2-[$^2H_4$]-choline substrates.

Data Analysis. The KaleidaGraph (Synergy Software, Reading, PA) and the Kinetic Studio Software Suite (Hi-TgK Scientific, Bradford on Avon, UK) were used to fit the kinetic data. Stopped-flow traces were best fit with the equation 1.

$$A = B\exp(-\lambda_1 t) + C\exp(-\lambda_2 t) + D \quad (1)$$

Equation 1 describes a double exponential process where λ_1 and λ_2 are the first order rate constants which represent the absorbance chance in the fast and slow phases, *t* is time, *A* is the absorbance at 450 nm at any given time, *B* and *C* are the amplitudes of the absorbance changes for the fast and slow phases, and *D* is the absorbance at infinite time. The kinetic parameters associated with the reductive half reaction (for fast and slow phases) were determined by using eq 2 and 3. The derivations of the equations were previously published and are not present here (*31*).

$$\lambda_1 = \frac{\lambda_{1lim}S+c}{{}^{app}K_{fast}+S} \quad (2)$$

$$\lambda_2 = \frac{\lambda_{2lim}S}{{}^{app}K_{slow}+S} \quad (3)$$

The observed first order rate constants are represented by λ_1 and λ_2 associated with absorbance change in the reduction of flavin in fast and slow kinetic phases respectively in eq. 1 and 2. S is any given concentration of the substrate, $\lambda_{1\text{lim}}$ and λ_{2lim} represent the limiting rate constants at saturated substrate concentration. The equilibrium between the enzyme and the substrate and the enzyme substrate complexes are dissociation constatnts and defined as ${}^{app}K_{\text{fast}}$ and ${}^{app}K_{\text{slow}}$. C is an offset value that accounts for nonzero absorbance value at infinite time.

$$\ln\left(\frac{k}{T}\right) = \left[\ln\left(\frac{k_B}{h}\right) + \frac{\Delta S^{\ddagger}}{R}\right] - \Delta H^{\ddagger}/RT \quad (4)$$

$$\ln(KIE) = \ln\left(\frac{A_H}{A_D}\right) - \left(\frac{\Delta E_a}{RT}\right) \quad (5)$$

Eyring's equation (eq 4) was used to fit with the limiting rate constants to analyze temperature dependence of proton and hydride transfer in CHO-S101A enzyme. k_B is the Boltzman constant and *h* is the Plank constant. The enthalpy of activation ($\Delta H^{\ddagger}$) is calculated from the slope, the entropy of activation ($\Delta S^{\ddagger}$) is calculated from the y-intercept of the plot. Arrhenius' equation (eq 5) was used to calculate the isotope effect on the Arrhenius' pre-factors (A_H/A_D)from the y-intercept and isotope effect on the activation energy (ΔE_a) from the slope of the plot.

2.3 Results

*Solvent and Substrate KIEs at 15 ^{o}C. S*olvent KIEs were determined with choline as substrate for the S101A variant of choline oxidase, to investigate the proton transfer reaction associated with choline oxidation catalyzed by the enzyme. The rate constants (λ) for anaerobic flavin reduction were determined in a stopped-flow spectrophotometer by mixing the enzyme with choline in 50 mM sodium pyrophosphate, pL 10.0 and 15 ^{o}C, and monitoring absorbance changes over time at 450 nm. The high pL was chosen because previous studies showed that at alkaline pH the catalytic steps associated with flavin reduction are independent of pL both in wild-type choline oxidase and a number of active site enzyme variants, such as E312D, H351A, H466A, H99N and S101A (H. Yuan & G. Gadda, unpublished data). Anaerobic mixing of the enzyme with choline resulted in the two-electron reduction of the enzyme-bound flavin (Figure 2.2-A), following a biphasic process (Figure 2.2-B). Accordingly the stopped-flow traces were fit best with a two-exponential process, defining fast (λ_1) and slow (λ_2) observed rate constants that were separated well (i.e., with $\lambda_1/\lambda_2 \geq 9$). Limiting values at saturating choline were determined for both the fast and slow kinetic phases by fitting the hyperbolic patterns of λ_1 and λ_2 as a function of choline concentration (Figure 2.2-C). In contrast, $^{app}K_D$ values could not be determined accurately since they were smaller than the lowest concentration of substrate that

could be used in the reaction while maintaining pseudo first-order conditions. For this reason the $^{app}K_D$ values are not reported. Replacement of water with deuterium oxide had large effects on the limiting value of λ_1 at saturating choline ($\lambda_{1(lim)}$), with values of 81 s^{-1} in H_2O and 18 s^{-1} in D_2O (Figure 2.2-C), yielding a solvent KIE of 4.5 on the fast kinetic phase seen in the stopped-flow spectrophotometer. In contrast, much smaller differences were seen on $\lambda_{2(lim)}$, for which the solvent KIE was 1.7 (Table 2.1). These results are in agreement with a recent study carried out at 25 ^oC showing solvent KIEs of 3.8 on λ_1 and 1.7 on λ_2, in which it was concluded that λ_1 is associated with the proton transfer reaction catalyzed by the S101A enzyme variant.

Substrate KIEs were determined with choline and 1,2-[$^2H_4$]-choline under the same conditions described above, in order to probe the hydride transfer reaction catalyzed by the S101A enzyme. While there were small differences in $\lambda_{1(lim)}$ upon substituting choline with deuterated choline, with values of 81 s^{-1} and 71 s^{-1}, large differences where seen in $\lambda_{2(lim)}$, with values of 3.1 s^{-1} and 0.4 s^{-1} (Figure 2.3). Thus, the substrate KIE was 1.1 on λ_1 and 8.3 on λ_2. These data agree well with previous results at 25 ^oC showing substrate KIEs of 1 on λ_1 and 6.5 on λ_2, in which it was concluded that λ_2 is associated with the hydride transfer reaction catalyzed by the S101A enzyme variant.

Effect of Temperature on the Proton Transfer Reaction. The effect of changing temperature on λ_1 and its associated solvent KIE was investigated to establish whether the proton transfer reaction catalyzed in the S101A enzyme variant occurs quantum mechanically. Anaerobic flavin reduction was investigated as described above, with choline as substrate and either water or deuterium oxide as buffered solvent at pL 10.0 in the temperature range from 15 ^oC to 39 ^oC. As expected, $\lambda_{1(lim)}$ increased with increasing temperature (Table 2.1) yielding linear dependencies when the data were analyzed by using the Eyring's formalism (Figure 2.4-A). The fit of the data

acquired in water and deuterium oxide to the Eyring's equation yielded lines with similar slopes and similar y-intercepts (Figure 2.4-A). Accordingly, the $^{D2O}\lambda_{1(lim)}$ values were comprised between 3.4 and 5.3 (Table 2.2), with a temperature independent average solvent KIE of 4.4. From the Eyring's analysis of the temperature dependence of $\lambda_{1(lim)}$, the enthalpy ($\Delta H^{\ddagger}$), entropy ($\Delta S^{\ddagger}$), and Gibbs free energy ($\Delta G^{\ddagger}$) of activation for the proton and deuteron transfer reactions catalyzed by the S101A enzyme were calculated (Table 2.3). The Arrhenius analysis of the temperature dependence of $\lambda_{1(lim)}$ was used to calculate the difference in the energy of activation for proton transfer in water and deuterium oxide (ΔE_a) and the isotope effect on the Arrhenius prefactors (A_H/A_D) (Table 2.3). Figure 2.4-B shows the temperature dependence of the $^{D2O}\lambda_{1(lim)}$ values, 1.9 ± 0.8 kcal/mol value of ΔE_a from the slopes and 112 ± 30 value of A_H/A_D were calculated from the y-intercepts of the lines.

Effect of Temperature on the Hydride Transfer Reaction. The effect of changing temperature on λ_2 and its associated substrate KIE was investigated to establish if hydride transfer in the S101A enzyme occurs within a highly preorganized enzyme-substrate complex as in the case of the wild-type enzyme (*10*). Anaerobic substrate reduction was investigated as described above with choline and 1,2-[$^2H_4$]-choline as substrate in aqueous buffer at pH 10.0 in the temperature range from 15 ^{o}C to 39 ^{o}C. When the $\lambda_{2(lim)}$ values were treated according to the Eyring's formalism, the protiated substrate yielded a line with a negative slope larger than that of the deuterated substrate (Figure 2.5), yielding an unprecedented increase in the measured $^{D}\lambda_{2(lim)}$ values determined through rapid kinetics with increasing temperature (Table 2.2).

It is well established that measured KIEs, including the $^{D}\lambda_{2(lim)}$ values determined here, may be affected by kinetic complexity, thereby not reflecting *per se* the intrinsic KIEs that would be required to draw mechanistic conclusions (*33*). Consequently, substrate KIEs determined using

the steady-state kinetic approach were used here as a tool to establish whether kinetic complexity affected the reductive half-reaction of the S101A enzyme. The steady-state kinetic parameters k_{cat} and $k_{cat}/K_{choline}$ were determined at pH 10.0 by measuring initial rates of oxygen consumption at varying concentrations of choline or 1,2-[$^2H_4$]-choline and oxygen, and the resulting KIEs were computed. As shown in Table 2.3, the $^{D}k_{cat}$ values were larger than the $^{D}(k_{cat}/K_m)$ values at 15, 23, 31 and 37 ^{o}C (Table 2.4), consistent with kinetic complexity in the reductive half-reaction being manifest in substrate KIEs. A commitment (C_f) value was calculated by using $^{D}k_{cat}$ and $^{D}(k_{cat}/K_m)$ values for each temperature at 15, 23, 31 and 37 ^{o}C by using the equation 6 in order to address the kinetic complexity. Intrinsic KIEs were calculated from observed KIEs and the calculated C_f values by using equation 7 [both equation 6 and 7 are from (*34*)] (Table 2.5). The Arrhenius analysis of $^{D}\lambda_{2(lim)}$ by using calculated intrinsic values showed temperature independent behavior as seen in Figure 2.5.

$$C_f = \frac{D_{(k_{cat})} - D_{(k_{cat}/K_m)}}{D_{(k_{cat}/K_m)} - 1} \quad (6)$$

$$KIE_{obs} = \frac{KIE_{int} + C_f}{1 + C_f} \quad (7)$$

2.4 Discussion

Temperature dependence of deuterium kinetic isotope effects was used to investigate the quantum mechanical behavior of proton and hydride transfer in the CHO-S101A variant. The reductive half-reaction in choline oxidase S101A mutant follows substrate proton abstraction from hydroxyl group of choline then hydride transfer from the α-carbon of choline alkoxide species to the flavin N(5) atom where betaine aldehyde forms as an intermediate. Evidence for this conclusion comes from large KIEs of 4.4 on fast phase (λ_1) and smaller KIEs of 1.7 on slow phase (λ_2) when water was substituted with deuterium oxide. In contrast, large KIEs of 8.3 on λ_2

and smaller KIEs of 1.1 on λ_1 were observed when choline was substituted with 1,2-[$^2H_4$]-choline. These results are consistent throughout the temperature range between 15 and 39 ^oC and in agreement with previously published data at 25^oC in CHO-S101A enzyme (*31*) which indicates a stepwise mechanism for proton then the hydride transfer at all temperatures were tested.

The proton transfer in the reductive half-reaction of CHO-S101A enzyme occurs within a preorganized active site via quantum tunneling. Evidence supporting this conclusion came from Eyring and Arrhenius analysis. Similar enthalpy and entropy of activations and same Gibbs free energies for proton and deuteron transfer were calculated from Eyring's analysis (Table 2.3). The similarity in thermodynamic parameters rules out the transition state model for this reaction where higher $\Delta H^{\ddagger}$ and $\Delta G^{\ddagger}$ are expected for the heavy isotope transfer compared to the light isotope due to zero point energy differences (*1, 2, 8*). This conclusion is also supported by the temperature independent KIEs in CHO-S101A enzyme. The activation energy difference for proton transfer in water and deuterium oxide (ΔE_a) was calculated as close to unity as well as highly inflated value of KIEs on Arrhenius pre-factors (A_H/A_D), such behavior does not agree with the classical models and supporting the quantum tunneling behavior. According to the Bell tunneling model, in enzymatic reactions with no tunneling the A_H/A_D value approaches unity (range of 0.8 to 1.4) (*9*).

A possible explanation for the value of A_H'/A_D' (determined by taking the ratio of y-intercepts of Eyring's plot) is being slightly higher than unity (1.5 ± 0.1) could be due to a higher viscosity coming from deuterated solvent versus to protiated solvent. These data indicating that different protein dynamics manifested from D_2O or H_2O might be affecting the limiting rate constants for the proton transfer reaction. Interestingly, a similar value (average of 1.4 ± 0.1) was observed for

$^{D2O}\lambda_2$ which reflects the isotope effects on the hydride transfer (expected value is 1) when isotopic substitution is made for the hydroxyl proton (proton in solvent with water and deuteron in solvent with deuterium oxide) (Table 2.1). The data suggest that the protein dynamics might be affected by the increased viscosity of deuterated solvent with respect to the solvent with water, which may lower the limiting rate constant for the hydride transfer. Interestingly, averaged 1.1 ± 0.1 value of $^{D}\lambda_1$ value was determined for the proton transfer when choline is substituted with 1,2-[$^2H_4$]-choline, both reactions were carried out in H_2O providing equal solvent conditions that is affecting the protein dynamics.

In contrast, temperature dependence on the KIEs of hydride transfer showed ambiguous results in CHO-S101A enzyme. According to the Eyring's analysis (Figure 2.5) kinetic isotope effects were determined to be an average of ≥ 14 at high temperature regime (≥ 25 ^{o}C) and an average of KIEs of ≤ 8 at low temperature regime (< 25 ^{o}C) (Table 2.2). The reduced KIEs at low temperatures arise from kinetic complexity in the reductive half-reaction catalyzed by CHO-Ser101Ala. A possible conformational change in enzyme-substrate complex would mask the intrinsic kinetic isotope effects where such conformational change is not present in the high temperature regime (alternatively, present with a different extent between low and high temperatures). Evidence supporting this conclusion came from steady-state kinetics where substrate KIEs were determined to address possible kinetic complexity affecting intrinsic KIEs in CHO-S101A enzyme.

In order to elucidate the unusual behavior of temperature dependence of KIEs of hydride transfer observed in CHO-Ser101Ala, $^{D}k_{cat}$ and $^{D}(k_{cat}/K_{choline})$ values at 15, 23, 31 and 37 ^{o}C were determined. KIEs determined with steady-state kinetic approach could be used as a tool to show the presence of commitment to catalysis (*33*). In this study, significantly lower $^{D}(k_{cat}/K_{choline})$

values than the $^{D}k_{cat}$ were determined at low and high temperature regimes in the reductive half-reaction (Table 2.4). An internal equilibrium could arise from conformational change influencing the enzyme-substrate complex. Such behavior results in lower $^{D}(k_{cat}/K_{choline})$ values, thereby, decreasing the intrinsic KIEs (*33, 35, 36*). Such internal equilibrium described here was previously proposed in CHO-Glu312Asp where deprotonation of the alcohol substrate yields an alkoxide species results in a conformational change that is associated with the enzyme-substrate complex (*29*).

It was previously published that in the presence of kinetic complexity $^{D}k_{cat}$ and $^{D}(k_{cat}/K_{choline})$ values can be used to calculate the commitment (C_f) value that affects the intrinsic KIEs (*34*). Temperature dependent C_f values and independent KIE_{int} values were calculated at 15, 23, 31 and 37 ^{o}C by using this approach (Table 2.5) [for these calculations eq 4 and 5 were used from reference (*34*)]. The Arrhenius analysis of temperature dependence of KIE_{int} values ($^{D2O}\lambda_2$) for the hydride transfer indicated that this reaction occurs via quantum mechanical tunneling as it is in the wild type choline oxidase (*10*). The evidences for this conclusion came from large A_H/A_D value of 32 ± 17 and small 1.4 ± 4.6 value of ΔE_a for the hydride and deuteride transfer in the CHO-S101A enzyme (Figure 2.5).

The proton transfer reaction in the wild-type enzyme was shown to occur in the dead time of the stopped-flow instrument (2.2 ms) and a lower value of 1900 s^{-1} for limiting rate constant was estimated at 25 ^{o}C . In this study, fast phases (λ_1) for the proton and deuteron transfer were observed in the stopped flow traces for all temperatures tested (Table 2.4). Since the proton transfer has been shown to occur via quantum mechanical tunneling in CHO-Ser101Ala enzyme, it is plausible to assume that the wild type enzyme should have a tunneling mechanism for proton transfer as well. A possible explanation for ~12 fold decrease in the limiting rate constant for

proton transfer in CHO-Ser101Ala enzyme could be the internal equilibrium due to conformational change that affecting the enzyme-substrate complex. Evidences supporting this conclusion came from significantly lower $^{D}(k_{cat}/K_{choline})$ values with respect to $^{D}k_{cat}$ values suggesting that such conformational chance would affect the limiting rate constant for the proton transfer.

In conclusion, according to Eyring's and Arrhenius analysis the proton transfer in CHO-Ser101Ala enzyme occur via quantum mechanical tunneling. This conclusion suggested that the proton transfer in the wild type may also occur via tunneling; fast proton transfer could not be determined due to the experimental limitations in wild type choline oxidase (*31*). In contrast, this study showed that a kinetic complexity manifested in the reductive half-reaction, determined with rapid the kinetic approach, may lower the intrinsic KIEs for the hydride transfer. Calculated intrinsic KIEs showed temperature independence that indicates quantum tunneling for the hydride transfer. It was established that solvent viscosity might affect the tunneling reaction by altering fast protein motions not only in the active site microenvironment but affecting the motions in entire protein (*37*, *38*). In this study, similar values for isotope effects on Eyring's prefactors (A_H'/A_D') and hydride transfer ($^{D2O}\lambda_2$) when water substituted with deuterium oxide suggested that viscosity of the solvent might affect the reaction catalyzed in CHO-S101A. These data provide evidence for fast protein motions might be coupling with the reaction coordinate. Overall, substitution of Ser101 with alanine in choline oxidase did not change the quantum mechanical tunneling for proton (assuming that the proton transfer occurs via quantum tunneling in the wild type) and hydride transfer reactions but an internal equilibrium of the enzyme substrate complex due to a conformational change that is relevant for catalysis manifests itself in mutant enzyme but not in the wild type.

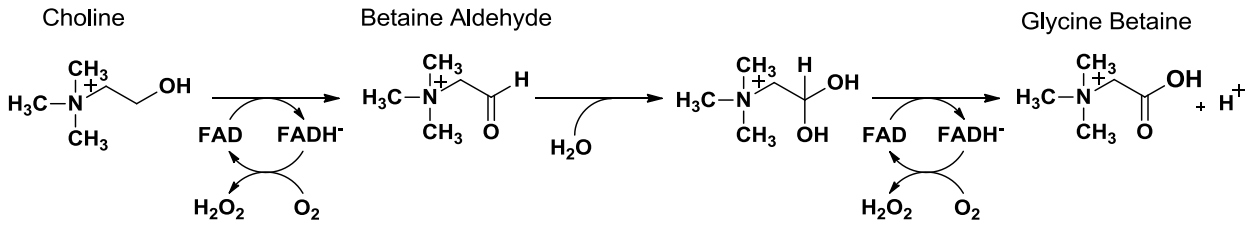

Scheme 2.1. Oxidation of Choline Catalyzed by Choline Oxidase

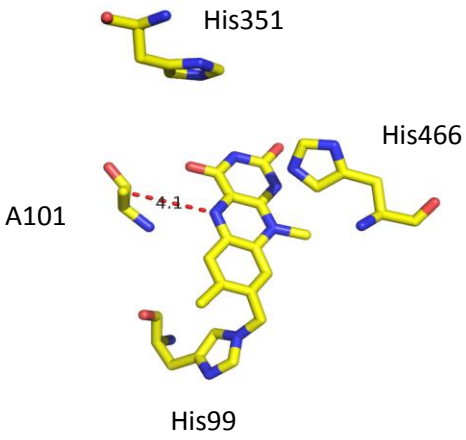

Figure 2.1. The X-ray structure of the CHO-Ser101Ala active site showing the distance between Ala101 and the N(5) atom of the flavin. The structure is from Protein Data Bank entry 3NNE. Yellow color represents carbon, red represents oxygen and blue represents nitrogen atoms.

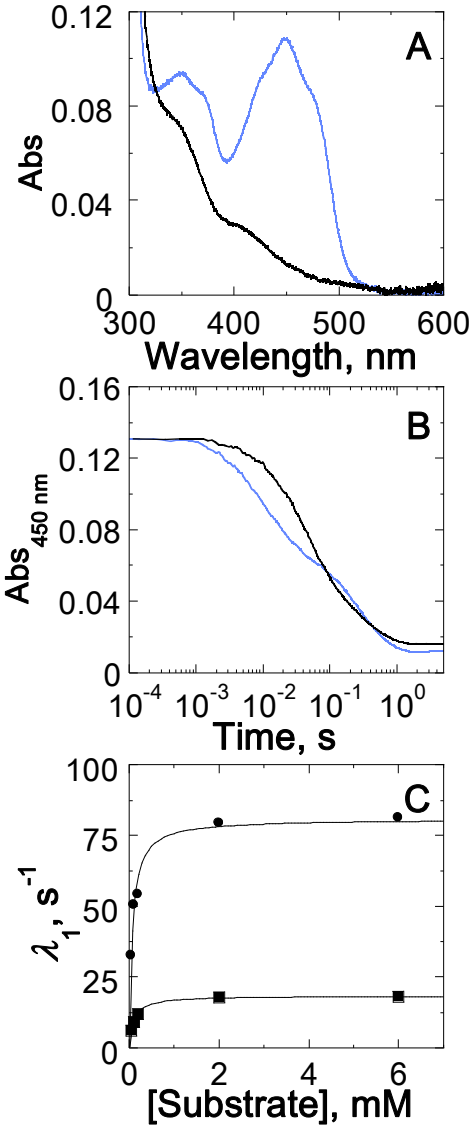

Figure 2.2. The reduction of enzyme bound flavin in the CHO-S101A enzyme in anaerobic conditions. The experiments were carried out in 50 mM sodium pyrophosphate (pL 10.0) at 15 ^{o}C. (A) UV-visible absorbance spectra obtained in saturated substrate concentration (6 mM choline in H_2O or D_2O). Oxidized enzyme (blue) and reduced enzyme (black). (B) Stopped-flow traces of choline in H_2O (black) and in D_2O (blue) obtained in saturated substrate concentration (6 mM choline in H_2O or D_2O). Data fit with eq 1. (C) Observed rate constants for proton transfer reaction in CHO-S101A enzyme as a function of choline in H_2O (circles) and D_2O (squares). Data fit with eq 2.

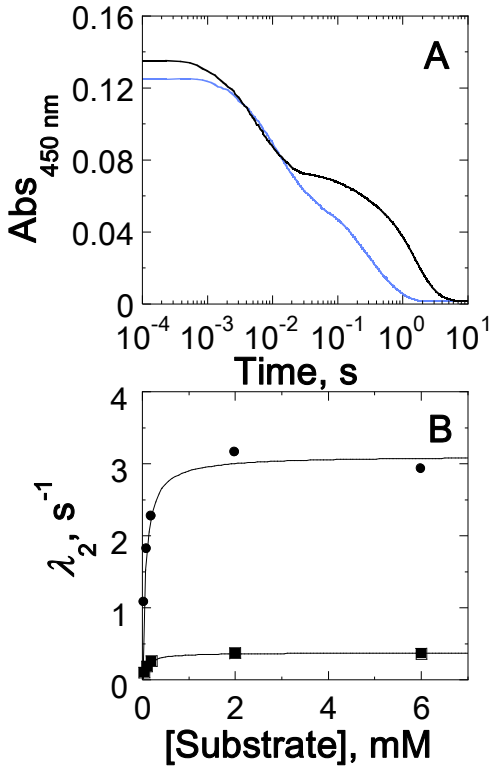

Figure 2.3. The reduction of enzyme bound flavin in the CHO-S101A enzyme in anaerobic conditions. The experiments were carried out in 50 mM sodium pyrophosphate (pH 10.0) at 15 ^{o}C. (A) Stopped-flow traces of choline (blue) and 1,2-[2H4]-choline (black) obtained in saturated substrate concentrations ~6mM. Data fit with eq 1. (B) Observed rate constants for hydride transfer reaction in CHO-S101A enzyme as a function of choline (circles) and 1,2-[$^{2}H_4$]-choline (squares). Data fit with eq 2.

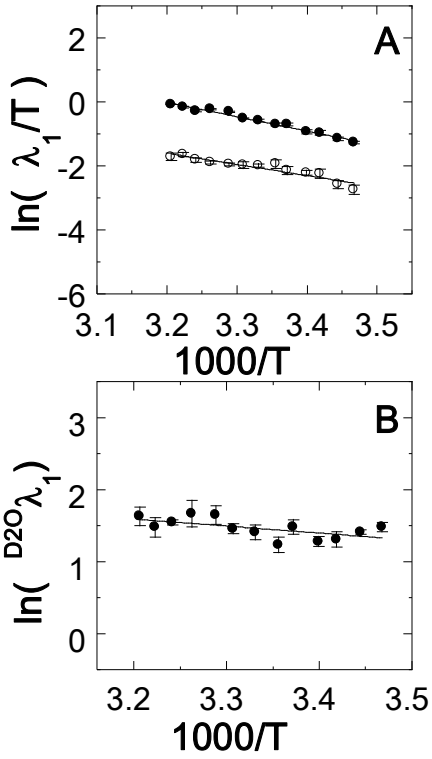

Figure 2.4. Temperature dependence of λ_1/T (Panel A) with choline in H_2O (black circles) choline in D_2O (white circles). Temperature dependence of $^{D2O}\lambda_1$ (Panel B). Rapid kinetic assays were performed in 50 mM sodium pyrophosphate at pL 10.0 with varying concentrations of substrates from 0.04mM to 6 mM in anaerobic conditions. The temperature range was selected from 15 ^{o}C to 37 ^{o}C. All data used in the plots are in Table S1 in the Supporting information.

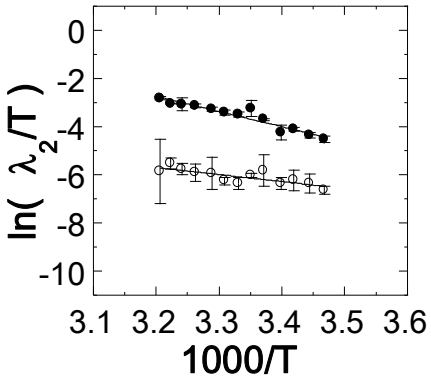

Figure 2.5. Temperature dependence of λ_2/T (Panel A) with choline in H_2O (black circles), with 1,2-[$^2H_4$]-choline (white circles).

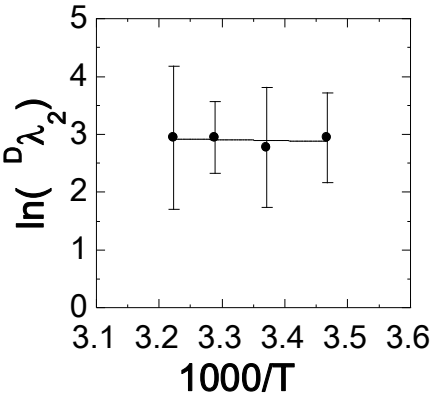

Figure 2.6. Temperature dependence of hydride transfer in the CHO-Ser101Ala ($^D\lambda_2$) with calculated intrinsic isotope effects.

Table 2.1. The limiting rate constants for proton transfer (λ_1) and the hydride transfer (λ_2) in CHO-S101A

	choline, H_2O		1,2-[$^2H_4$]-choline, H_2O		choline, D_2O	
Temperature (^oC)	$\lambda_1(s^{-1})$	$\lambda_2(s^{-1})$	$\lambda_1(s^{-1})$	$\lambda_2(s^{-1})$	$\lambda_1(s^{-1})$	$\lambda_2(s^{-1})$
39	289 ± 14	18.6 ± 0.5	300 ± 24	0.88 ± 0.20	56 ± 4	9.3 ± 1.0
37	263 ± 20	14.8 ± 0.1	279 ±13	1.25 ± 0.05	60 ± 2	10.5 ± 0.5
35	233 ± 21	14.3 ± 1.2	170 ± 1	0.97 ± 0.04	50 ± 2	7.5 ± 0.7
33	245 ± 28	13.3 ± 0.4	192 ± 20	0.82 ± 0.05	46 ± 1	9.3 ± 0.5
31	221 ± 14	11.5 ± 0.3	190 ± 4	0.80 ± 0.09	43 ± 1	7.8 ± 0.1
29	180 ± 5	10.0 ± 0.3	175 ± 10	0.85 ± 0.02	42 ± 2	9.4 ± 0.6
27	167 ± 11	9.1 ± 0.3	168 ± 13	0.52 ± 0.02	41 ± 1	7.3 ± 0.3
25	148 ± 9	11.5 ± 1.2	128 ± 7	0.72 ± 0.01	43 ± 3	21 ± 3
23	146 ± 7	7.3 ± 0.1	129 ± 9	0.88 ± 0.10	35 ± 2	5.5 ± 0.7
21	116 ± 8	4.2 ± 0.3	115 ± 4	0.51 ± 0.02	32 ± 1	2.6 ± 0.2
19	111 ± 8	4.8 ± 0.1	110 ± 5	0.58 ± 0.04	31 ± 2	4.1 ± 0.2
17	92 ± 4	3.7 ± 0.1	82 ± 3	0.50 ± 0.03	22 ± 1	3.3 ± 0.1
15	81 ± 3	3.1 ± 0.1	71 ± 2	0.38 ± 0.01	18 ± 1	1.9 ± 0.1

Conditions : 50 mM sodium pyrophosphate, pL 10.0 in anaerobic conditions

Table 2.2. Kinetic isotope effects on fast (λ_1) and slow (λ_2) phases

T ^{o}C	$^{D}\lambda_1$ [a]	$^{D}\lambda_2$ [a]	$^{D2O}\lambda_1$ [b]	$^{D2O}\lambda_2$ [b]
39	1.0 ± 0.1	21 ± 5.0	5.1 ± 0.4	2.0 ± 0.1
37	1.0 ± 0.1	12 ± 0.5	4.4 ± 0.4	1.4 ± 0.1
35	1.4 ± 0.1	15 ± 1.0	4.7 ± 0.1	1.9 ± 0.1
33	1.3 ± 0.2	16 ± 1.0	5.3 ± 0.6	1.4 ± 0.1
31	1.2 ± 0.1	14 ± 2.0	5.2 ± 0.4	1.5 ± 0.1
29	1.0 ± 0.1	12 ± 0.5	4.3 ± 0.2	1.1 ± 0.1
27	1.0 ± 0.1	17 ± 1.0	4.1 ± 0.3	1.2 ± 0.1
25	1.2 ± 0.1	16 ± 1.7	3.4 ± 0.3	0.5 ± 0.1
23	1.1 ± 0.1	8.0 ± 0.3	4.4 ± 0.3	1.3 ± 0.1
21	1.0 ± 0.1	8.3 ± 0.2	3.6 ± 0.2	1.6 ± 0.1
19	1.0 ± 0.1	8.2 ± 0.6	3.7 ± 0.3	1.2 ± 0.1
17	1.1 ± 0.1	7.5 ± 0.4	4.1 ± 0.1	1.2 ± 0.1
15	1.1 ± 0.1	8.3 ± 0.3	4.4 ± 0.2	1.7 ± 0.1
Average	1.1 ± 0.1	nd	4.4 ± 0.3	1.4 ± 0.1

Conditions: 50 mM sodium pyrophosphate at pL 10. [a] $^{D}\lambda_{1\&2}$ values were determined by using choline and 1,2-[$^{2}H_4$]choline. [b] $^{D2O}\lambda_{1\&2}$ values determined by using choline in H_2O and D_2O.

Table 2.3. Thermodynamic parameters for proton transfer catalyzed by CHO-S101A

CHO-S101A	
	$^{D2O}\lambda_1$
A_H/A_D[a]	112 ± 30
A_H'/A_D'[b]	1.5 ± 0.1
ΔE_a[a], kcal mol^{-1}	-1.9 ± 0.8
$\Delta H^{\ddagger}_H$[c], kcal mol^{-1}	8.8 ± 0.5
$\Delta H^{\ddagger}_D$[c], kcal mol^{-1}	7.2 ± 0.5
$\Delta S^{\ddagger}_H$[c], kcal mol^{-1}	0.020 ± 0.001
$\Delta S^{\ddagger}_D$[c], kcal mol^{-1}	0.028 ± 0.004
$\Delta G^{\ddagger}_H$, kcal mol^{-1}	14 ± 0.5
$\Delta G^{\ddagger}_D$, kcal mol^{-1}	15 ± 1.2

Conditions: 50 mM sodium pyrophosphate , pL 10 in anaerobic conditions. [a]A_H/A_D and ΔE_a values were determined by using the Arrhenius equation. [b]A_H'/A_D' value was calculated by taking the ratio of y-intercepts from the Eyring's plot. [c]Data were calculated by using the Eyring's equation (eq 4)

Table 2.4. KIEs determined with steady state approach for CHO-S101A

T ^{o}C	$^{D}(k_{cat})$	$^{D}(k_{cat}/K_{m})$
15	9.5 ± 0.5	4.5 ± 0.9
23	8.0 ± 0.6	4.3 ± 1.6
31	7.1 ± 0.2	5.2 ± 0.8
37	9.8 ± 0.4	6.6 ± 1.2

Conditions: Steady state parameters were determined with choline and 1,2-[$^{2}H_{4}$]choline in 50 mM sodium pyrophosphate at pH 10. Various concentrations of substrate used within the range from 0.05 to 6 mM.

Table 2.5. Observed and intrinsic KIEs for hydride transfer inCHO-S101A

T ^{o}C	KIE_{obs}	C_f	KIE_{int}
15	8.3 ± 0.3	1.40 ± 0.60	19 ± 5
23	8.0 ± 0.3	1.10 ± 0.70	16 ± 6
31	14 ± 2.0	0.40 ± 0.18	19 ± 4
37	12 ± 0.5	0.60 ± 0.25	19 ± 8

C_f and KIE_{int} values calculated with equations 6 and 7 from reference (34).

2.5. References

1. Nagel, Z. D., and Klinman, J. P. (2010) Update 1 of: Tunneling and dynamics in enzymatic hydride transfer, *Chem Rev 110*, PR41-67.
2. Klinman, J. P. (2006) Linking protein structure and dynamics to catalysis: the role of hydrogen tunnelling, *Philos Trans R Soc Lond B Biol Sci 361*, 1323-1331.
3. Nagel, Z. D., Meadows, C. W., Dong, M., Bahnson, B. J., and Klinman, J. P. (2012) Active site hydrophobic residues impact hydrogen tunneling differently in a thermophilic alcohol dehydrogenase at optimal versus nonoptimal temperatures, *Biochemistry 51*, 4147-4156.
4. Hay, S., Johannissen, L. O., Hothi, P., Sutcliffe, M. J., and Scrutton, N. S. (2012) Pressure effects on enzyme-catalyzed quantum tunneling events arise from protein-specific structural and dynamic changes, *J Am Chem Soc 134*, 9749-9754.
5. Heyes, D. J., Sakuma, M., de Visser, S. P., and Scrutton, N. S. (2009) Nuclear quantum tunneling in the light-activated enzyme protochlorophyllide oxidoreductase, *J Biol Chem 284*, 3762-3767.
6. Schwartz, S. D., and Schramm, V. L. (2009) Enzymatic transition states and dynamic motion in barrier crossing, *Nat Chem Biol 5*, 551-558.
7. Nagel, Z. D., and Klinman, J. P. (2006) Tunneling and dynamics in enzymatic hydride transfer, *Chem Rev 106*, 3095-3118.
8. Knapp, M. J., and Klinman, J. P. (2002) Environmentally coupled hydrogen tunneling. Linking catalysis to dynamics, *Eur J Biochem 269*, 3113-3121.
9. Bell, R. P. (1980) *The tunnel effect in chemistry*, Chapman and Hall, London ; New York.

10. Fan, F., and Gadda, G. (2005) Oxygen- and temperature-dependent kinetic isotope effects in choline oxidase: correlating reversible hydride transfer with environmentally enhanced tunneling, *J Am Chem Soc 127*, 17954-17961.

11. Pudney, C. R., Johannissen, L. O., Sutcliffe, M. J., Hay, S., and Scrutton, N. S. (2010) Direct analysis of donor-acceptor distance and relationship to isotope effects and the force constant for barrier compression in enzymatic H-tunneling reactions, *J Am Chem Soc 132*, 11329-11335.

12. Meyer, M. P., Tomchick, D. R., and Klinman, J. P. (2008) Enzyme structure and dynamics affect hydrogen tunneling: the impact of a remote side chain (I553) in soybean lipoxygenase-1, *Proc Natl Acad Sci U S A 105*, 1146-1151.

13. Sharma, S. C., and Klinman, J. P. (2008) Experimental evidence for hydrogen tunneling when the isotopic arrhenius prefactor (A(H)/A(D)) is unity, *J Am Chem Soc 130*, 17632-17633.

14. Bahnson, B. J., Park, D. H., Kim, K., Plapp, B. V., and Klinman, J. P. (1993) Unmasking of hydrogen tunneling in the horse liver alcohol dehydrogenase reaction by site-directed mutagenesis, *Biochemistry 32*, 5503-5507.

15. Kohen, A., Cannio, R., Bartolucci, S., and Klinman, J. P. (1999) Enzyme dynamics and hydrogen tunnelling in a thermophilic alcohol dehydrogenase, *Nature 399*, 496-499.

16. Hay, S., Pudney, C. R., Sutcliffe, M. J., and Scrutton, N. S. (2010) Probing active site geometry using high pressure and secondary isotope effects in an enzyme-catalysed 'deep' H-tunnelling reaction, *J Phys Org Chem 23*, 696-701.

17. Brinkley, D. W., and Roth, J. P. (2005) Determination of a large reorganization energy barrier for hydride abstraction by glucose oxidase, *J Am Chem Soc 127*, 15720-15721.

18. Fan, F., and Gadda, G. (2005) On the catalytic mechanism of choline oxidase, *J Am Chem Soc 127*, 2067-2074.

19. Gadda, G. (2008) Hydride transfer made easy in the reaction of alcohol oxidation catalyzed by flavin-dependent oxidases, *Biochemistry 47*, 13745-13753.

20. Gadda, G. (2003) Kinetic mechanism of choline oxidase from Arthrobacter globiformis, *Biochim Biophys Acta 1646*, 112-118.

21. Gadda, G. (2003) pH and deuterium kinetic isotope effects studies on the oxidation of choline to betaine-aldehyde catalyzed by choline oxidase, *Biochim Biophys Acta 1650*, 4-9.

22. Ghanem, M., Fan, F., Francis, K., and Gadda, G. (2003) Spectroscopic and kinetic properties of recombinant choline oxidase from Arthrobacter globiformis, *Biochemistry 42*, 15179-15188.

23. Ghanem, M., and Gadda, G. (2005) On the catalytic role of the conserved active site residue His466 of choline oxidase, *Biochemistry 44*, 893-904.

24. Ghanem, M., and Gadda, G. (2006) Effects of reversing the protein positive charge in the proximity of the flavin N(1) locus of choline oxidase, *Biochemistry 45*, 3437-3447.

25. Rungsrisuriyachai, K., and Gadda, G. (2009) A pH switch affects the steady-state kinetic mechanism of pyranose 2-oxidase from Trametes ochracea, *Arch Biochem Biophys 483*, 10-15.

26. Rungsrisuriyachai, K., and Gadda, G. (2010) Role of asparagine 510 in the relative timing of substrate bond cleavages in the reaction catalyzed by choline oxidase, *Biochemistry 49*, 2483-2490.

27. Quaye, O., Cowins, S., and Gadda, G. (2009) Contribution of flavin covalent linkage with histidine 99 to the reaction catalyzed by choline oxidase, *J Biol Chem 284*, 16990-16997.

28. Quaye, O., and Gadda, G. (2009) Effect of a conservative mutation of an active site residue involved in substrate binding on the hydride tunneling reaction catalyzed by choline oxidase, *Arch Biochem Biophys 489*, 10-14.

29. Quaye, O., Lountos, G. T., Fan, F., Orville, A. M., and Gadda, G. (2008) Role of Glu312 in binding and positioning of the substrate for the hydride transfer reaction in choline oxidase, *Biochemistry 47*, 243-256.

30. Quaye, O., Nguyen, T., Gannavaram, S., Pennati, A., and Gadda, G. (2010) Rescuing of the hydride transfer reaction in the Glu312Asp variant of choline oxidase by a substrate analogue, *Arch Biochem Biophys 499*, 1-5.

31. Yuan, H., and Gadda, G. (2011) Importance of a serine proximal to the C(4a) and N(5) flavin atoms for hydride transfer in choline oxidase, *Biochemistry 50*, 770-779.

32. Finnegan, S., Yuan, H., Wang, Y. F., Orville, A. M., Weber, I. T., and Gadda, G. (2010) Structural and kinetic studies on the Ser101Ala variant of choline oxidase: catalysis by compromise, *Arch Biochem Biophys 501*, 207-213.

33. Cleland, W. W. (1982) *The use of isotope effects to determine transition-state structure for enzymic reactions*, Vol. 87, Methods Enzymology.

34. Klinman, J. P. (2013) Importance of Protein Dynamics during Enzymatic C-H Bond Cleavage Catalysis, *Biochemistry*.

35. Grissom, C. B., and Cleland, W. W. (1988) Isotope effect studies of the chemical mechanism of pig heart NADP isocitrate dehydrogenase, *Biochemistry 27*, 2934-2943.

36. Emanuele, J. J., and Fitzpatrick, P. F. (1995) Mechanistic studies of the flavoprotein tryptophan 2-monooxygenase. 2. pH and kinetic isotope effects, *Biochemistry 34*, 3716-3723.

37. Loveridge, E. J., Evans, R. M., and Allemann, R. K. (2008) Solvent effects on environmentally coupled hydrogen tunnelling during catalysis by dihydrofolate reductase from Thermotoga maritima, *Chemistry 14*, 10782-10788.

38. Pudney, C. R., Guerriero, A., Baxter, N. J., Johannissen, L. O., Waltho, J. P., Hay, S., and Scrutton, N. S. (2013) Fast protein motions are coupled to enzyme h-transfer reactions, *J Am Chem Soc 135*, 2512-2517.

CHAPTER 3.

CONCLUSIONS

3.1 Conclusions

The proton and hydride tunneling in an active site variant Ser101Ala of choline oxidase were investigated through temperature dependence on kinetic isotope effects. The results presented in this study showed that the proton transfer occurs via quantum tunneling in CHO-S101A according to the Eyring's and the Arrhenius' analysis. Previously, the tunneling behavior of hydride transfer was investigated in wild type choline oxidase at 25 ^{o}C (*1*), however, due to instrumental limitations and significantly high rate constants (estimated value 1900 s^{-1}) for proton transfer, this reaction could not be measured in wild type enzyme. Since the proton transfer occurs via tunneling in the CHO-S101A mutant enzyme, it is reasonable to assume that the wild type choline oxidase would also exhibit tunneling behavior for the same reaction.

Temperature dependence of KIEs for hydride tunneling in CHO-S101A showed an unusual behavior. The magnitude of KIEs was smaller at low temperature than high temperature regime. A possible explanation for such behavior could be that by introducing a mutation in the active site the donor-acceptor distance need not necessarily increased but may actually be decreased. In decreased donor-acceptor distances, the tunneling probability would be higher for both light and heavy isotopes which results in smaller KIEs (*2*). Alternatively, at low temperatures the active site motions can freeze out which makes distance sampling more difficult for both light and heavy isotopes (*3*). However, in some cases, a kinetic complexity might result in unexpected observations. The KIEs measured for hydride transfer in CHO-S101A decreased at low temperatures due to a kinetic complexity suggested by comparison of $^{D}(k_{cat})$ and $^{D}(k_{cat}/K_{m})$ values. This study showed that observed kinetic isotope effects determined with rapid kinetic

approach might not be equal to the intrinsic values. The hydride tunneling reaction occurs via quantum tunneling in CHO-S101A enzyme similar to the wild type as suggested by the temperature independent intrinsic kinetic isotope effects (KIE_{int} values were calculated by using the equations from (*4*)). In conclusion, substitution of Ser101 with alanine in choline oxidase did not change the quantum mechanical tunneling for proton (assuming that the proton transfer occurs via quantum tunneling in the wild type) and hydride transfer reactions but an internal equilibrium of the enzyme substrate complex due to a conformational change that is relevant for catalysis manifests itself in mutant enzyme but not in the wild type.

3.2. References

1. Fan, F., and Gadda, G. (2005) Oxygen- and temperature-dependent kinetic isotope effects in choline oxidase: correlating reversible hydride transfer with environmentally enhanced tunneling, *Journal of the American Chemical Society 127*, 17954-17961.
2. Pudney, C. R., Johannissen, L. O., Sutcliffe, M. J., Hay, S., and Scrutton, N. S. (2010) Direct analysis of donor-acceptor distance and relationship to isotope effects and the force constant for barrier compression in enzymatic H-tunneling reactions, *Journal of the American Chemical Society 132*, 11329-11335.
3. Nagel, Z. D., and Klinman, J. P. (2010) Update 1 of: Tunneling and dynamics in enzymatic hydride transfer, *Chemical reviews 110*, PR41-67.
4. Klinman, J. P. (2013) Importance of Protein Dynamics during Enzymatic C-H Bond Cleavage Catalysis, *Biochemistry*.